

SKYLAB/EREP APPLICATION TO ECOLOGICAL, GEOLOGICAL, AND OCEANOGRAPHIC INVESTIGATIONS OF DELAWARE BAY

(E78-10003) SKYLAB/EREP APPLICATION TO ECOLOGICAL GEOLOGICAL, AND OCEANOGRAPHIC INVESTIGATIONS OF DELAWARE BAY Final Report, Jun. 1973: - Mar. 1976 (Delaware Univ.) 68 p EC A04/MF A01	N78-12492 Unclas CSCI 08C G3/43 00003
---	---

Vytautas Klemas
David S. Bartlett
William D. Philpot

College of Marine Studies
University of Delaware
Newark, Delaware
19711

Robert H. Rogers
Larry E. Reed

Bendix Aerospace Systems Division
3300 Plymouth Road
Ann Arbor, Michigan
48107

May 1976
Final Report for Period June 1973-March 1976

CMS-NASA-1-76

Original photography may be purchased from:
EROS Data Center

Sioux Falls, SD

Prepared for
NASA Langley Research Center
Hampton, Virginia 23365

and

NASA L. B. Johnson Space Center
Houston, Texas 77058

Number of Investigation: Skylab/EREP Investigation 477
 Period Covered: June 5, 1973 - March 17, 1976
 Contract Number: NAS1-12304
 Principal Investigations Management Office: NASA Langley Research Center
 Technical Monitor: Robert W. Johnson
 Principal Investigator: Vytautas Klemas
 Sponsoring Institution: College of Marine Studies
 University of Delaware
 Type of Report: Final Report

ACKNOWLEDGMENT

In addition to the five authors of this report, the following individuals made contributions to this interdisciplinary effort:

- F. C. Daiber, Professor, Marine Biology
- G. R. Davis, Marine Scientist
- R. D. Henry, Staff Geohydrologist, Delaware Department of Natural Resources and Environmental Control
- R. Hicks, NASA Johnson Space Center
- R. Joosten, NASA Johnson Space Center
- R. W. Johnson, NASA Langley Research Center
- J. D. Koutsandreas, EPA Office of Research and Monitoring
- W. R. McCluney, NASA Goddard S.F.C., Physical Oceanography
- K.-H. Szekiolda, Assistant Professor, Chemical Oceanography
- H. Wang, Professor, Ocean Engineering
- C. A. Wethe, Engineer, Sediments Analysis

To all these contributors we express our sincere gratitude.

TECHNICAL REPORT STANDARD TITLE PAGE

1. Report No. Final 1	2. Government Accession No.	3. Recipient's Catalog No.	
4. Title and Subtitle SKYLAB/EREP APPLICATION TO ECOLOGICAL, GEOLOGICAL, AND OCEANOGRAPHIC INVESTIGATIONS OF DELAWARE BAY		5. Report Date	
		6. Performing Organization Code February 1976	
7. Author(s) V. Klemas, D. Bartlett, W. Philpot; R. Rogers, L. Reed*;		8. Performing Organization Report No.	
9. Performing Organization Name and Address College of Marine Studies University of Delaware Newark, Delaware 19711		10. Work Unit No.	
		11. Contract or Grant No. NAS1-12304	
		13. Type of Report and Period Covered Final (Type III) June, 1973-March, 1976	
12. Sponsoring Agency Name and Address Dr. R. W. Johnson Langley Research Center National Aeronautics & Space Administration Hampton, Virginia 23365		14. Sponsoring Agency Code	
15. Supplementary Notes *R. Rogers and L. Reed Bendix Aerospace Systems Division Ann Arbor, Michigan 48107			
16. Abstract Skylab/EREP S190A and S190B film products have been optically enhanced and visually interpreted to extract data suitable for mapping coastal land use; inventorying wetlands vegetation; monitoring tidal conditions; observing suspended sediment patterns; charting surface currents; locating coastal fronts and water mass boundaries; monitoring industrial and municipal waste dumps in the ocean; determining the size and flow direction of river, bay and man-made discharge plumes; and observing ship traffic. Film products were visually analyzed to identify and map ten land-use and vegetation categories at a scale of 1:125,000. Comparison of these thematic maps with CARETS Land Use Maps resulted in classification accuracies ranging from 50% to 98%. Digital tapes from the S192 Multispectral Scanner were used to prepare thematic maps of land use. Classification accuracies obtained by comparison of S192 derived thematic maps of land use with USGS-CARETS land-use maps in southern Delaware ranged from 44% to 100%. The resolutions of the S190A, S190B and S192 systems were 20-40m, 10-20m, and 70-100m, respectively.			
17. Key Words (Selected by Author(s)) Coastal Remote Sensing Marsh Vegetation Mapping Coastal Land-Use Mapping Current Circulation Charting Pollution Dispersion Monitoring		18. Distribution Statement	
19. Security Classif. (of this report) Unclassified	20. Security Classif. (of this page) Unclassified	21. No. of Pages 67	22. Price*

*For sale by the Clearinghouse for Federal Scientific and Technical Information, Springfield, Virginia 22151.

TABLE OF CONTENTS

1.0	INTRODUCTION	7
2.0	DESCRIPTION OF THE DELAWARE BAY TEST SITE	8
2.1	Socio-Economic Characteristics of Delaware Bay	8
2.2	Physical Characteristics of Delaware Bay	11
3.0	ACQUISITION AND PROCESSING OF SKYLAB PHOTOGRAPHY AND DIGITAL DATA	16
4.0	S190A AND S190B FILM CAMERA RESULTS	25
4.1	Coastal Vegetation and Land Use	25
4.2	Coastal Processes and Water Properties	33
4.2.1	Suspended Sediment Patterns and Current Circulation	33
4.2.2	Spatial Resolution and Ship Traffic Monitoring	45
4.2.3	Observation of Ocean Waste Disposal Plumes	47
5.0	S192 MULTISPECTRAL SCANNER RESULTS	53
5.1	Test Site	53
5.2	Analysis Procedure	53
5.2.1	Screening of Raw Data	53
5.3	Results of Multispectral Classification	55
6.0	SUMMARY AND CONCLUSIONS	60
7.0	RECOMMENDATIONS	62
8.0	REFERENCES	63
9.0	LIST OF RELATED PUBLICATIONS	65

LIST OF ILLUSTRATIONS

Figure 2.1	Delaware Bay test site for Skylab/EREP investigations.	10
Figure 2.2	Delaware Bay bathymetry. Tongues of deeper water radiate from the entrance into the bay.	13
Figure 3.1	Coverage of Delaware Bay test site by S190A, S190B and S192 pass on September 12, 1973.	17
Figure 3.2	Delaware Bay region as viewed by thirteen spectral channels of the Skylab/EREP S192 multispectral scanner with its conical line scan pattern.	20
Figure 3.3	False color composites prepared from digital tapes of S192 multispectral scanner bands.	21
Figure 4.1	Skylab/EREP color photograph of the Delaware Bay region obtained with the S190A multispectral photographic facility on September 12, 1973.	23
Figure 4.2	Skylab/EREP color infrared photograph of the Delaware Bay region obtained with the S190A multispectral photographic facility on September 12, 1973.	24
Figure 4.3	Skylab/EREP photograph of the Delaware Bay region obtained with the S190B earth terrain camera on September 12, 1973.	26
Figure 4.4	Land-use map derived from Skylab/EREP image by visual photo-interpretation.	27
Figure 4.5	Photograph of Delaware Bay region obtained by Skylab/EREP S190A multispectral photographic facility on September 12, 1973 in the "green" band (0.5-0.6 microns).	32
Figure 4.6	Photograph of Delaware Bay region obtained by Skylab/EREP S190A multispectral photographic facility on September 12, 1973 in the "red" band (0.6-0.7 microns).	34
Figure 4.7	Photograph of Delaware Bay region obtained by Skylab/EREP S190A multispectral photographic facility on September 12, 1973 in the near-infrared band (0.8-0.9 microns).	35
Figure 4.8	Interpretative map of major water features visible in Skylab/EREP S190B photograph shown in Figure 4.5 (Track 43, Rev. 1747, September 12, 1973).	36

Figure 4.9	Interpretative map of major water features visible in Skylab/EREP S190A photograph shown in Figure 4.3 (Track 43, Rev. 1747, September 12, 1973).	37
Figure 4.10	Approximate tidal current conditions in Delaware Bay during the Skylab/EREP overpass on September 12, 1973 (maximum ebb at Delaware Bay entrance).	38
Figure 4.11	Predicted tidal currents and LANDSAT-1 MSS band 5 image of Delaware Bay taken on May 13, 1973 (maximum ebb at Delaware Bay entrance).	40
Figure 4.12	Predicted tidal currents and LANDSAT-1 MSS band 5 image of Delaware Bay taken on February 13, 1973 (one hour after maximum ebb at Delaware Bay entrance).	42
Figure 4.13	Predicted tidal currents and LANDSAT-1 MSS band 5 image of Delaware Bay taken on December 3, 1972 (one hour before maximum ebb at Delaware Bay entrance).	43
Figure 4.14	Microdensitometer traces of October 10, 1972, LANDSAT-1 imagery from Cape Henlopen, Delaware to Cape May, New Jersey, using MSS bands 4, 5, and 6.	44
Figure 4.15	Suspended sediment concentration may be derived from LANDSAT-1 image radiance and a limited number of water sample analyses.	46
Figure 4.16	Enlarged digital enhancement of acid waste plume imaged by LANDSAT-1 on January 25, 1973:	48
Figure 4.17	Enlarged LANDSAT MSS band 5 image of barge dumping acid wastes at DuPont Company's ocean waste dump site.	50
Figure 5.1	Test site for Skylab/EREP S192 MSS analysis.	52

1.0 INTRODUCTION

There is a need for information on the natural state of the Delaware Bay and its surroundings to serve as a basis for rational decision-making on utilization. This need is recognized by most of those concerned with the conservation, regulation, or development of Delaware's Coastal Zone. It is made more accurate by present and proposed projects destined to affect the system. Among these are: a number of offshore developments associated with deep-draft vessels, including offshore oil terminals; oil prospecting and mining activities along the Continental Shelf; the enlargement of the Chesapeake and Delaware Canal; the installation of waste treatment plants and nuclear generating stations; and general dredging and construction activities in the coastal zone.

All of these projects have supporting engineering studies associated with them and some have ecological surveys as well. The difficulty is that these studies have restricted themselves in the past to the immediate vicinity of a project and have not related to the bay as an interdependent system. Therefore, we have attempted to use Skylab/EREP along with aircraft, other spacecraft (LANDSAT) and ground sampling to help establish a baseline defining the present condition of the river, bay, and coastal zone as an interrelated system. Future studies will employ aircraft and other spacecraft to monitor changes from this baseline and to predict environmental impact resulting from future, more intense development.

The second Skylab crew made three EREP passes over the Delaware Bay test site, one of which produced imagery of high quality. During this Skylab overpass, ground truth was collected by teams in boats and in the marshes. The purpose of this report is to review our investigations of coastal vegetation, land use, suspended sediment and current circulation patterns, and dispersion of wastes dumped in the ocean based on visual interpretation and digital analysis of Skylab/EREP data products.

2.0 DESCRIPTION OF THE DELAWARE BAY TEST SITE

Delaware Bay is an estuary on the eastern coast of the United States, bordered by the states of New Jersey and Delaware and situated between the major estuaries of New York Harbor and Chesapeake Bay. The geography of this region, including the locations of several convenient reference points, is shown in Figures 2.1 and 2.2. The SKYLAB/EREP Delaware Bay test site extends from 38°00'N to 40°00'N in latitude and from 74°00'W to 76°00'W in longitude.

2.1 Socio-Economic Characteristics of Delaware Bay

The Delaware River and Bay form the water gateway to a great industrial and commercial complex of the Delaware Valley. The coastal bays of Delaware are part of a system of shallow-water estuaries which are the nursery and rearing ground for most fin fishes important to both commercial and sport fishermen along the eastern coast of the United States. In fact, about two-thirds of the fish landed by U.S. fishermen spend part of their lives in an estuary. The tidal wetlands in Delaware, encompassing about 115,000 acres, are an important link in these grounds and provide breeding areas for birds, mammals, and shellfish; they produce food for all of these and are part of the aesthetic quality of the shore region.

The Atlantic Ocean, Delaware Bay, and other coastal bays and their surroundings are prime attractions for persons seeking water-based recreation adjacent to the east coast megalopolis. When considered together with the general absence of other significant topographic features and the lack of traditional mineral resources, Delaware Bay and other coastal bays represent not just a factor in the state's geography, but a determining factor in its history, economy, and way of life.

However, the Delaware Bay Region is threatened by the impact of rapid industrial and domestic development.¹ Adjacent to the Delaware Estuary is one of the major oil refining areas in the eastern part of the United States. Seven oil companies operate large refineries whose combined daily through-put is about 900,000 barrels or 3,780 million gallons. As of 1967, the Federal Water Quality Administration estimated that traffic of cargo ships, barges, naval vessels, and tankers on the Delaware exceeded 200 vessels per day, many of which either use petroleum

products or are involved in refinery operations, thereby contributing to oil spillage. Oil slicks involving surface patches of oil exceeding 1,000 feet in length and 50 angstroms in thickness, are recorded during routine sampling runs. During 1970, oil slicks were reported in 33 of 38 runs. Although few catastrophic spills have been recorded in the area in recent years, the growing literature on the biological effects of oil in aquatic systems points to significant insidious incorporation of hydrocarbons in the marine food chain as the result of low level chronic pollution.

The petrochemical, utility, and other industries are discharging increasing amounts of oil, exotic chemicals, and trace metals, as well as thermal effluent, all of which upset the ecology of the bay and its estuaries. For instance, in the foam along water boundaries we have found toxic metals, such as mercury and lead, at concentrations two to four orders of magnitude greater than the averages for Delaware Bay water.² A study of trace metals in bottom sediments near shellbanks in Delaware Bay concluded that iron, zinc, lead, cadmium, mercury, and nickel have their primary sources in the Delaware River, with high concentrations accumulating near the mouths of the Cohansey, Murderkill, and St. Jones Rivers.³

Waste disposal in the waters of the Delaware drainage system has been one of the foremost historical abuses of the environment. In 1964, it was estimated that 76,000 pounds per day of the Delaware River's ultimate oxygen demand was contributed by storm-water overflows. As a result of the chemical and biological oxygen demands, decreased oxygen levels are observed in the river near Philadelphia. In fact, anaerobic conditions persist over a 10-mile stretch of the river during the summer months. Obviously this low-to-zero oxygen band can eliminate anadromous fish spawning runs involving shad, sturgeon, and others. Additionally, nutrient enrichment occurs involving nitrate reduction to nitrite under anaerobic conditions and high phosphate levels. The combination of oxygen depletion and nutrient enrichment has a predictably debilitating effect on aquatic ecosystems.

Other ventures of man producing environmental impacts are major dredging projects, thermal additions due to power plant cooling needs,

ORIGINAL PAGE IS
OF POOR QUALITY

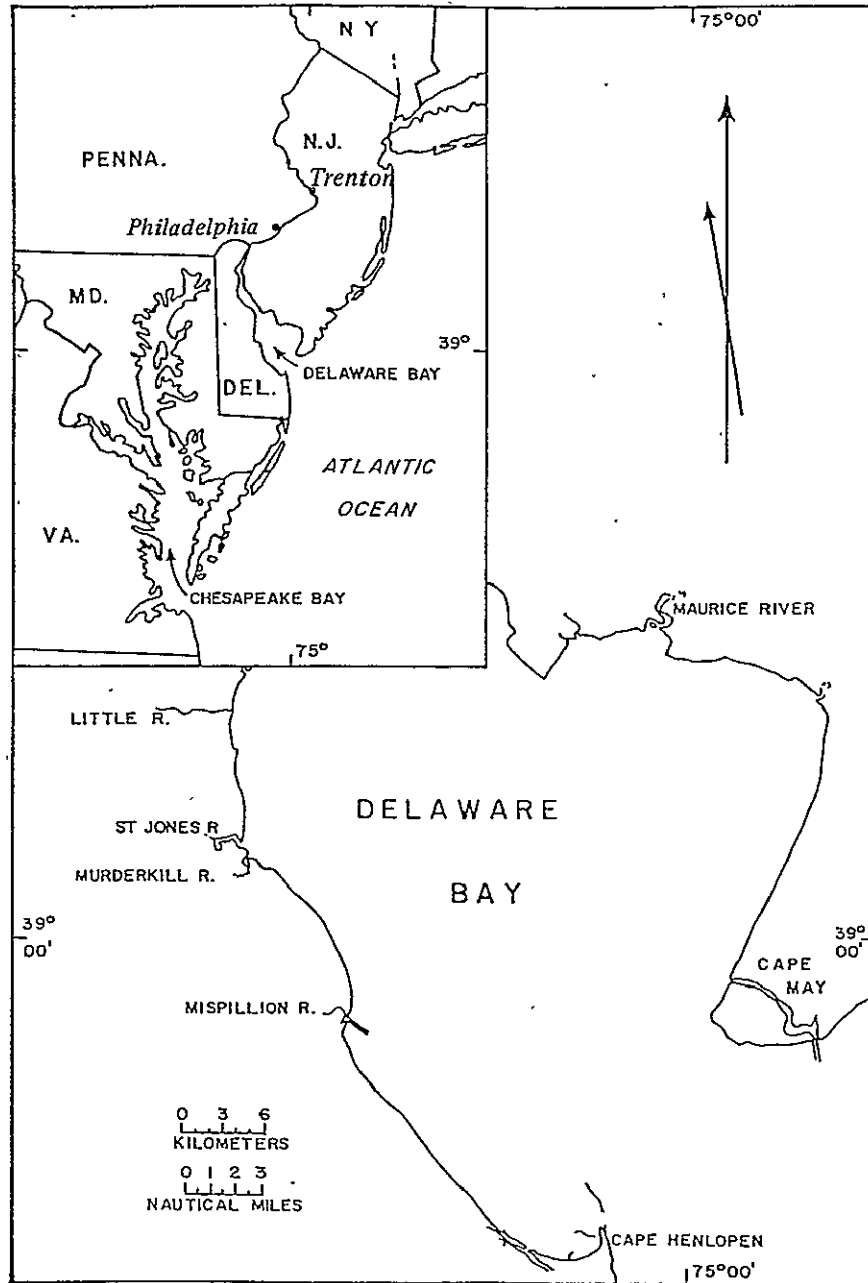


Figure 2.1 Delaware Bay test site for Skylab/EREP investigations

use of pesticides, sediment production, and diversion of fresh water from the headwaters of the Delaware.

Economic development of this coastal region has presented public officials and planners with difficult environmental and land-use problems; yet information on ecological deterioration in the region is difficult to acquire by conventional survey methods. The instantaneous areal distribution, and the variations in flow rate of waters from various sources, the unique meteorological conditions along the seacoast, and the variety of land uses and land forms that exist from the tidal zone to the upland hinterlands all combine to present a highly complex picture. This is complicated further by human activity, especially activities which involve emissions into the air and water, and by the widespread reworking of the land and the shoreline that has resulted from increasingly intensive land use. Of particular concern are plans for offshore oil terminals, sewage and power plants, dredging and commercial marsh development, which threaten to further degrade the coastal environment unless the environmental impact of each is carefully assessed and extrapolated in area and time.

We have found that remote sensing techniques offer an opportunity for simultaneous observation and measurement of large-scale features, their associated spectral patterns, their distribution, and spatial and temporal variance relative to the natural environment and to centers of man's activities. Since Skylab offers an excellent platform for earth observation, the objective of our overall program was to determine which coastal resource and environmental characteristics its sensors could discriminate; whether baseline thematic maps could be prepared by aerial extrapolation from a minimum of ground truth; and whether one could then proceed to a more operational mode to study natural and man-made changes from this baseline with spacecraft providing repetitive coverage of our test site.

2.2 Physical Characteristics of Delaware Bay

If Trenton, New Jersey, is taken to define the upper limit of the estuary, the total length of the estuary is over 200 kilometers (Figure 2.1). Delaware Bay itself may be distinguished as a less extensive body

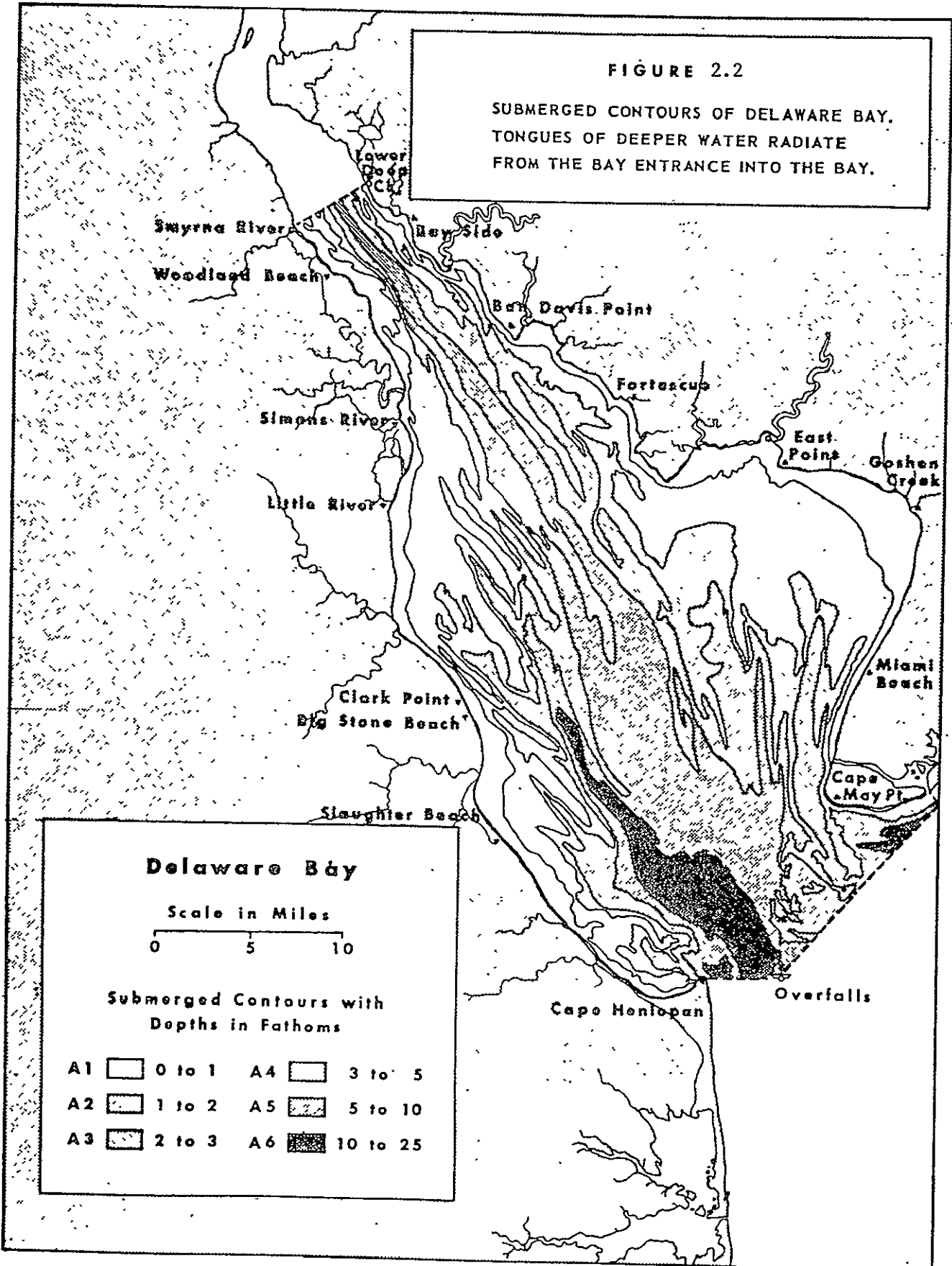
of water by defining an upper limit in the vicinity of the Smyrna River entrance (Figure 2.2). The length of the bay is 75.2 km, with mean and maximum widths of 24.6 km and 43.6 km respectively. The bay encompasses approximately 1864.8 sq. km and has a volume of about 1.78×10^{13} liters.

Fresh water input to the system is derived mainly from the Delaware River at an average rate of 316 cu.m/sec which, in terms of volume flow, ranks this as one of the major tributaries on the east coast. Together with this large volume of fresh water, the river also discharges a heavy load of suspended and dissolved material, since its effective watershed encompasses an area typified by intensive land use, both agricultural and industrial.⁴ Seaward of the Smyrna River, the bay undergoes a conspicuous exponential increase in both width and cross-sectional area so that the strength of the river flow is rapidly diminished beyond this point. Ketchum has computed the flushing time of the bay (defined in this case as the time required to replace the total fresh water volume of the bay) to be roughly 100 days.⁵ Seasonal variations in river flow cause this figure to fluctuate within a range of from 60 to 120 days. Consequently, river flow is not a significant factor in determining the current pattern in the bay except in the consideration of time-averaged flow. In terms of short-period studies it is mainly important as a source of suspended sediment and contaminants.

The seaward boundary of the bay extends from Cape May southeast to Cape Henlopen -- a distance of eleven miles. Tidal flow across this boundary profoundly affects the dynamic and hydrographic features of the entire estuary. The effect is especially pronounced toward the mouth where conditions are generally well mixed. The dynamic behavior of the tides is closely approximated by the model described by Harleman.⁶ In this model, the upper end of the estuary is assumed to act as an efficient reflecting boundary. Consequently, the actual tidal elevation at any given point is a result of the interaction of both a landward-directed wave entering from the ocean and a reflected wave traveling back down the estuary. The tidal range is a maximum at the reflecting boundary and decreases toward the mouth in a manner dependent upon the relative phase of the two components. Observations of the tide at Trenton show a 2.3 m range compared to a 1.2 m range at the mouth. A relative maximum appears

FIGURE 2.2

SUBMERGED CONTOURS OF DELAWARE BAY.
TONGUES OF DEEPER WATER RADIATE
FROM THE BAY ENTRANCE INTO THE BAY.



at roughly the location of Egg Island Point, where the phase relationship is temporarily optimal. An important consequence of this behavior is the occurrence of strong reversing tidal currents in the Delaware River. The tidal wavelength, as compared by Harleman, is 330 kilometers, so that both peak currents and slack water may occur simultaneously at either end of the bay.

In general, waters of the Delaware Bay circulate in a large rotary current, which normally flows southward along the western shore and northward along the eastern New Jersey shore. Due to the Coriolis effect, the flood tide reinforces the northerly flow component while the ebb tide reinforces the southerly current. During the flood tide, the maximum tidal current reaches 4.3 km/hr and 4.4 km/hr northwestward at the Cape May and Cape Henlopen entrance, respectively. During ebb tide, the maximum exit velocity reaches 5.0 km/hr and 5.2 km/hr southeast at Cape May and Cape Henlopen, respectively. Levels of 1.2 meters above the mean high water have been caused by extratropical cyclones. Strong easterly and southeasterly winds sometimes contribute to higher tides in the bay, resulting in the flooding of lowlands.

The tidal flow is also modified by the bay's rather complex bathymetry (Figure 2.2). Most prominent are several deep finger-like channels which extend from the mouth into the bay for varying distances.⁷ Depths of up to 46 meters are present, making this one of the deepest natural embayments on the east coast. The channels alternate with narrow shoals in a pattern which is shifted noticeably toward the southern shore. On the northern side, a broad, shallow mudflat extends from Cape May to Egg Island Point. Considerable transverse tidal shears result from these radical variations in bottom contour. As a consequence, a marked gradient structure may form perpendicular to the main axis of the bay as a function of tidal phase. This intrinsic two-dimensional character, together with the complex superimposed time variations, represents an almost insurmountable task when it is confronted with the tools of conventional hydrographic surveys. The problem is ready-made, however, for the techniques of high-altitude photography.

There are approximately 115,000 acres of tidal wetlands in the State of Delaware forming an almost continuous band along the western shore of

Delaware Bay from Cape Henlopen north to Wilmington. The width of this band varies from a few hundred yards to three to four miles, with an average width on the order of one mile. In addition, there are small fringes of marsh associated with the barrier beach-lagoon complexes along the Atlantic shore in the southern portion of the state.⁶ The most abundant plant species found in the marshes are salt marsh cord grass (Spartina alterniflora) salt marsh hay (Spartina patens), spike grass (Distichlis spicata) and reed grass (Phragmites communis).

There are, of course, many other species present but in most cases their occurrence is limited to small patches scattered within areas dominated by one or more of the above-mentioned primary species. In the north, Delaware's coastal zone is dominated by heavy industrial development, while its Atlantic coastline is feeling pressure from recreational builders.

3.0 ACQUISITION AND PROCESSING OF SKYLAB PHOTOGRAPHY AND DIGITAL DATA

The Earth Resources Experiment Package (EREP) was activated during the following three Skylab passes over the Delaware Bay region: August 5, 1973 (Track 61, Revolution 1197), September 12, 1973 (Track 43, Revolution 1747), and September 17, 1973 (Track 43, Revolution 1818). On September 17 Skylab and ERTS-1 imaged our test site within 9 minutes of each other. However, of the three Skylab/EREP attempts only the pass on September 12, 1973 produced imagery free of major cloud cover.

The Skylab/EREP data products evaluated include magnetic tapes from the multispectral scanner (S192) containing thirteen spectral bands ranging from 0.4 to 12.5 microns; a 5-inch format color transparency from the S190B Earth Terrain Camera; and six sets of 70-mm positive transparencies from the S190A Multispectral Photographic facility, including color, color infrared, and four additional bands in the visible and near IR spectral range (Table 3.1). From an altitude of 435 km, each S190A camera frame was imaging an area of 163 x 163 km.

TABLE 3.1

S190A Multispectral Photography Bands

Camera Station	Film	Filter	Spectral Band (μ)
Camera 1	2424	CC	0.7-0.8
Camera 2	2424	DD	0.8-0.9
Camera 3	3443	EE	0.5-0.88
Camera 4	SO-242	FF	0.4-0.7
Camera 5	3400	BB	0.6-0.7
Camera 6	3400	AA	0.5-0.6

The exact coverage of the Delaware Bay test site by the S190A, S190B, and S192 systems during the pass on September 12, 1973, is shown in Figure 3.1. The Atlantic coast from Maryland to New Jersey was well covered by all three systems. However, only the S190A covered the entire

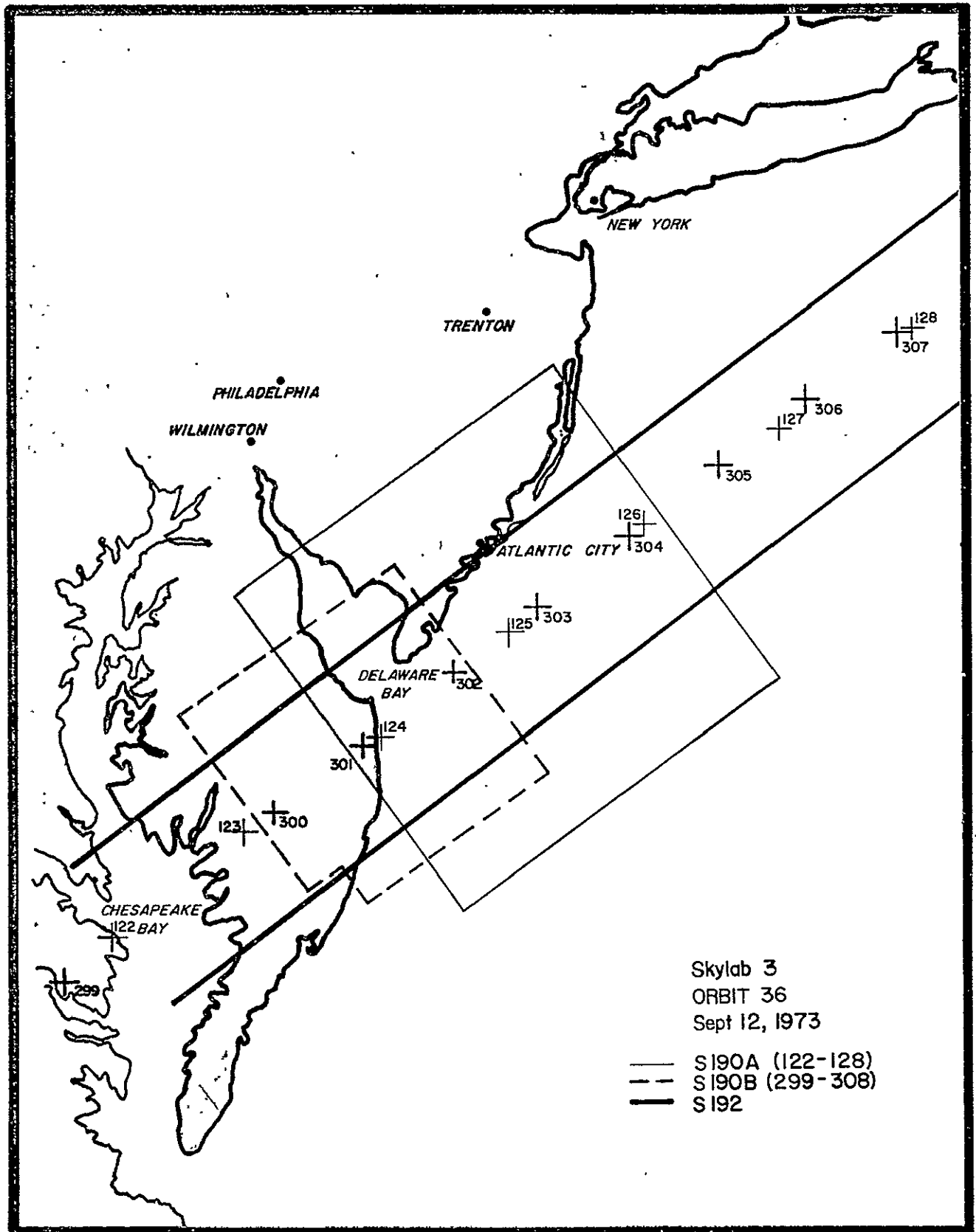


Figure 3.1 Coverage of Delaware Bay test site by S190A, S190B, and S192 systems during Skylab/EREP pass on September 12, 1973

Delaware Bay, while the S190B covered half of the bay and the S192 only the mouth of the bay between Cape May and Cape Henlopen.

Imagery and digital tapes from twelve LANDSAT passes over Delaware Bay have been also analyzed as part of another program. The LANDSAT imagery used in our work was produced by the four-channel multispectral scanner having the bands shown in Table 3.2. From an altitude of 920 km, each frame covered an area of 186 x 198 km. In addition to the 9-track 800 bpi magnetic tapes, reconstructed negative and positive transparencies in 70 mm format and prints in 9-inch format were obtained from NASA. Before visual interpretation, some of the imagery was enhanced optically, using density slicing and color additive techniques. Annotated thematic maps were prepared by computer analysis of digital tapes and by direct photointerpretation of the transparencies reconstructed by NASA.

TABLE 3.2

EREP S192 and ERTS MSS Bands

S192		LANDSAT	
Band No.	Band (μ)	Band (μ)	Band No.
1	0.41-0.46		
2	0.46-0.51		
3	0.52-0.56		
4	0.56-0.61	0.5-0.6	4
5	0.62-0.67	0.6-0.7	5
6	0.68-0.76		
7	0.78-0.88	0.7-0.8	6
8	0.98-1.08		
9	1.09-1.19	0.8-1.1	7
10	1.20-1.30		
11	1.55-1.75		
12	2.10-2.35		
13	10.2-12.5		

The most notable difference between the SKYLAB S192 and LANDSAT MSS sensor characteristics is the larger number of S192 bands, thirteen as compared to four in MSS; and the S192's swath width (72.3 km) which covers approximately one-half of the distance covered by LANDSAT (185 km). A scene of Delaware and Delaware Bay acquired by the S192 on September 12, 1973 is shown in Figure 3.2. Table 3.2 provides S192 band locations and notes corresponding LANDSAT bands. In S192 band 1 a general lack of contrast was observed. This is due to both low atmospheric transmission and radiance reflected back into the scanner from the atmosphere (path radiance). False color composites prepared from the original digital tapes of the S192 multispectral scanner are shown in Figure 3.3.

Two sets of S192 tapes were obtained from NASA in response to the University's requests. The first set of S192 data was recorded on a high density digital tape (HDDT) having 10,000 bpi. As explained in the next paragraph, when the HDDT were analyzed, various noise patterns were observed in the imagery. Therefore a second "noise-filtered" set of S192 data was requested from NASA in the standard computer compatible tape (CCT) format, on a nine-track 800 bpi tape.

Another notable fact is the conical-line scan pattern used by the S192. Single-band imagery produced directly from the HDDT has this same conical pattern, making identification of small targets (based on spatial features) somewhat difficult (Figure 3.2).

The original S192 HDDT data had to be preprocessed before any usable data products could be generated. These steps include (a) transferring raw data from HDDT to standard 9-track CCT, and (b) using this tape to generate another tape whose data is "linearized" (i.e., as if the scan were normal to the direction of spacecraft motion). This data although linearized still has distortions due to earth rotation.

The various noise patterns observable in many of the original S192 bands are another notable feature.⁸ Noise characteristics observed in the unfiltered S192 imagery were as follows:

Detector Noise: Detector noise is a very low frequency (f) noise source. It has a $1/f$ characteristic. It shows up as a slow variation in scanner gain and offset and is most noticeable in thermal band 13. It could be removed by referencing the two calibration sources and

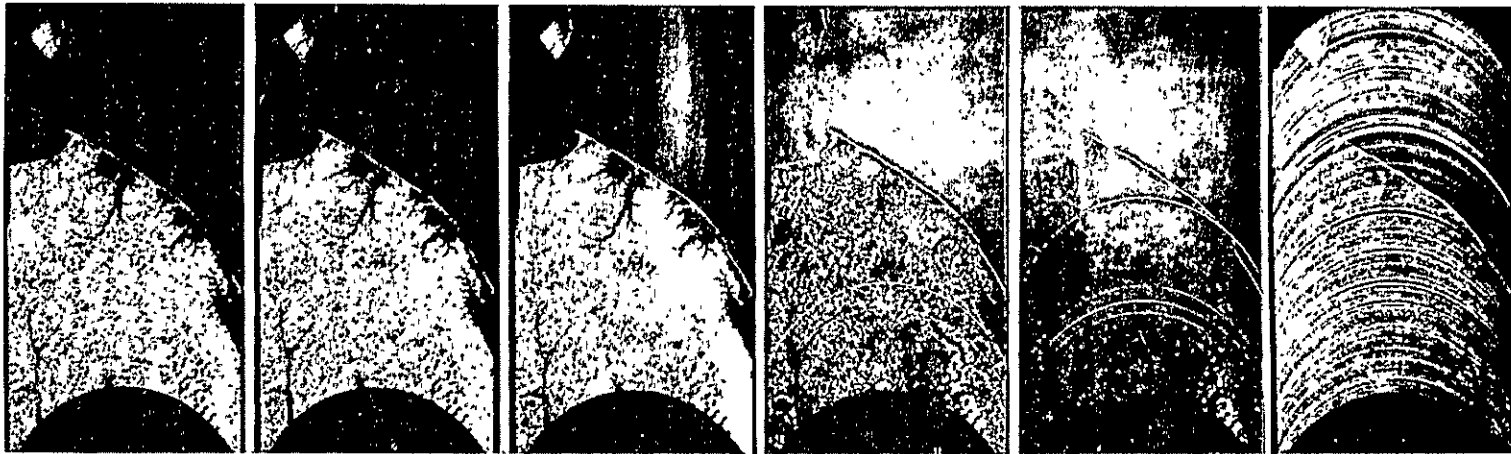
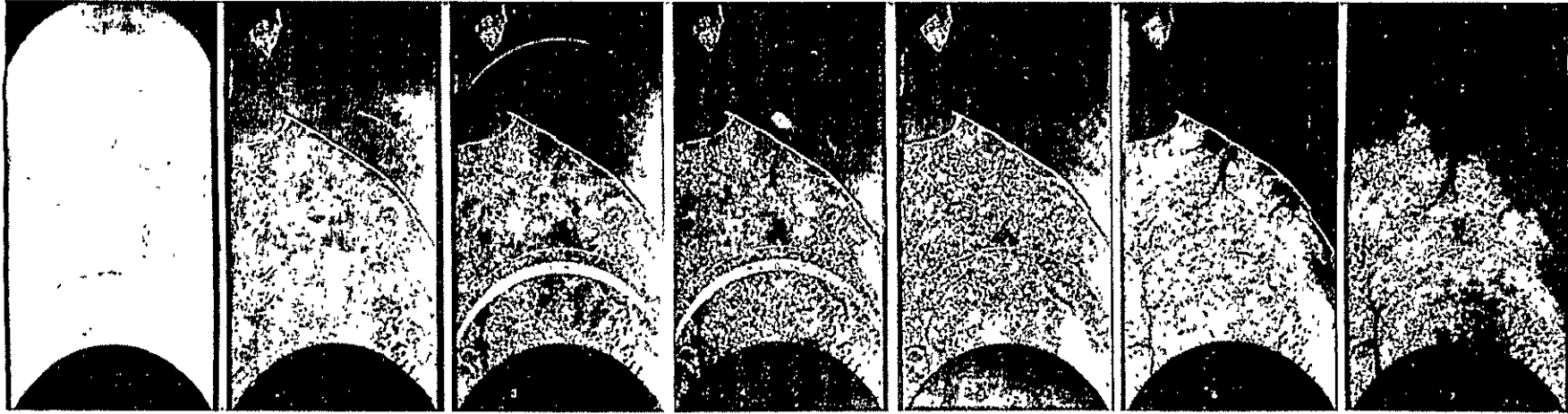


Figure 3.2 Delaware Bay region as viewed by thirteen spectral channels of the Skylab/EREP S192 multispectral scanner with its conical line scan pattern

ORIGINAL PAGE IS
POOR QUALITY

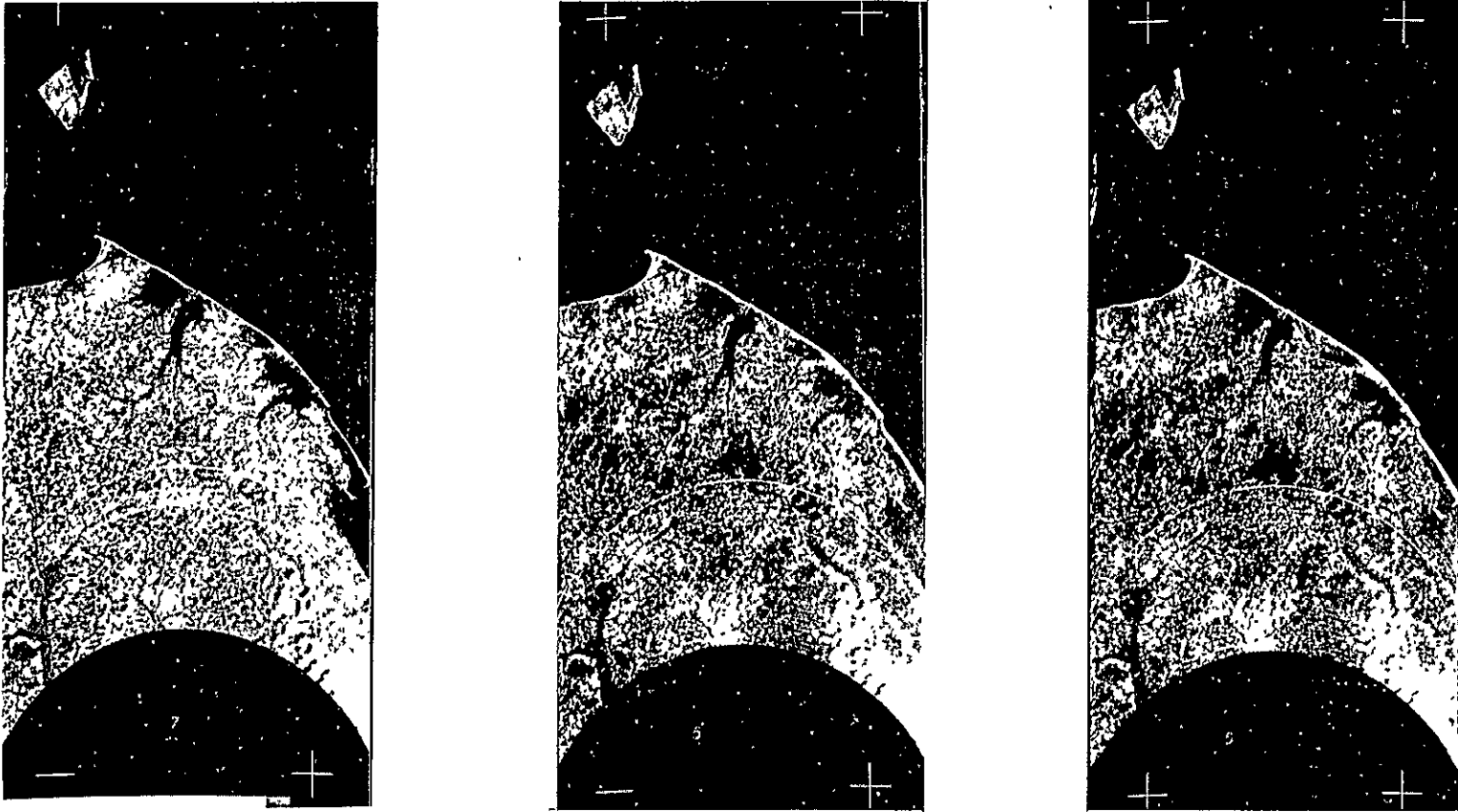


Figure 3.3 False color composites prepared from digital tapes of S192 multispectral scanner bands

ORIGINAL PAGE IS
OF POOR QUALITY

determining what gain and offset to add to the calibration signals (also to the video) to force them to remain at a constant level.

Cooler Piston Noise: Most noticeable noise over Delaware Bay is in band 5. It has a fundamental frequency in the range 16-18 Hz (i.e., a period of about 6 scan lines). It could be removed by simulating a notch filter.

Power Inverter: The power inverter produces a herringbone pattern which requires close analysis over homogeneous areas (e.g., water). It has a fundamental frequency whose period is approximately 16 resolution elements. It could also be removed by digital simulation of a notch filter. This noise is most noticeable in band 4, and to some extent in bands 1, 2, 3, 5, 7, and 8.

Sync Drop-Outs: Poor signal-to-noise ratio on sync signal causes the film recorder to lose timing signal, resulting in the major banding observed in bands 3 and 4.

Noise problems have been studied intensively by NASA. Noise-filtered tapes were delivered to investigators and used in our analysis of S192 imagery.

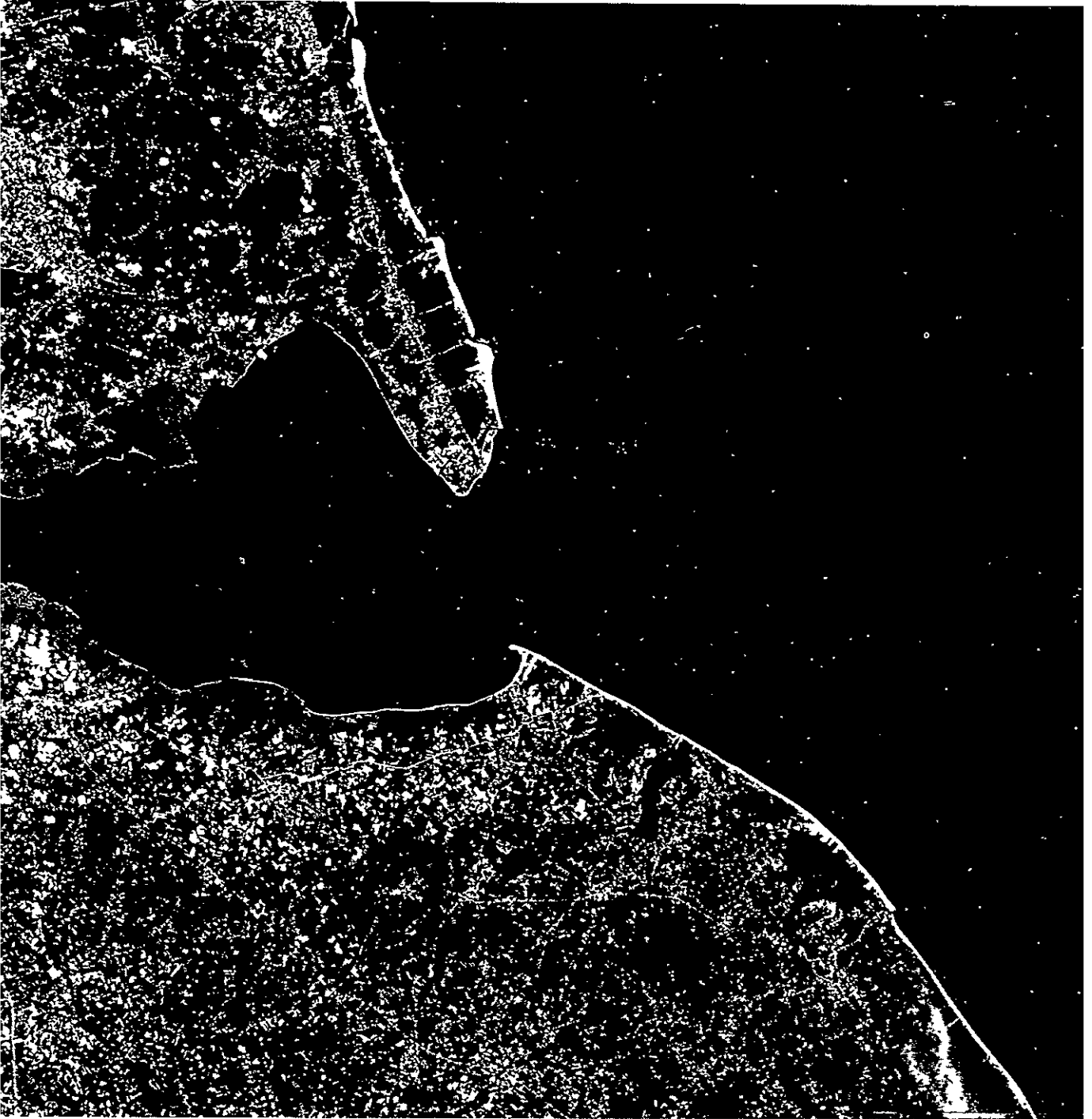


Figure 4.1 Skylab/EREP color photograph of the Delaware Bay region obtained with the S190A multispectral photographic facility on September 12, 1973



Figure 4.2 Skylab/EREP color infrared photograph of the Delaware Bay region obtained with the S190A multispectral photographic facility on September 12, 1973

4.0 S190A AND S190B FILM CAMERA RESULTS

4.1 Coastal Vegetation and Land Use

Skylab/EREP photos were visually analyzed using the Bausch and Lomb "Zoom Transfer Scope".⁸ The 5-inch, S190B, color photograph (see Figure 4.3) was used, primarily because it offered the best spatial resolution. Enlargements of the 70mm, S190A, color infrared photo (see Figure 4.2) were used to supplement the analysis, particularly where more detailed definition of water boundaries and vegetation species was required. Ten land-use and vegetation categories, as listed in Table 4.1, were manually identified based on color, size, shape, location, contrast and other factors, and mapped at a scale of 1:125,000 (see Figure 4.4).

TABLE 4.1

Vegetation and Land-Use Categories

-
1. Forest land
 2. Spartina alterniflora
 3. Cropland
 4. Plowed cropland
 5. Sand and bare sandy soil
 6. Deep saline water
 7. Sediment-laden and shallow saline water
 8. Built-up land
 9. Tended grass (including golf courses, etc.)
 10. Dunes and beach grass
-

Several subcategories of cropland could be seen but were not mapped in this initial attempt. Cartographic quality appeared to be very good as no anamorphic corrections were required in the scale matching and map overlay procedure performed with the "Zoom Transfer Scope." Resolution of the S190B image (10-20m) appears compatible with map accuracy standards for maps at scales of 1:100,000 or smaller, although at this stage no attempt has been made to conform to those standards in thematic mapping.

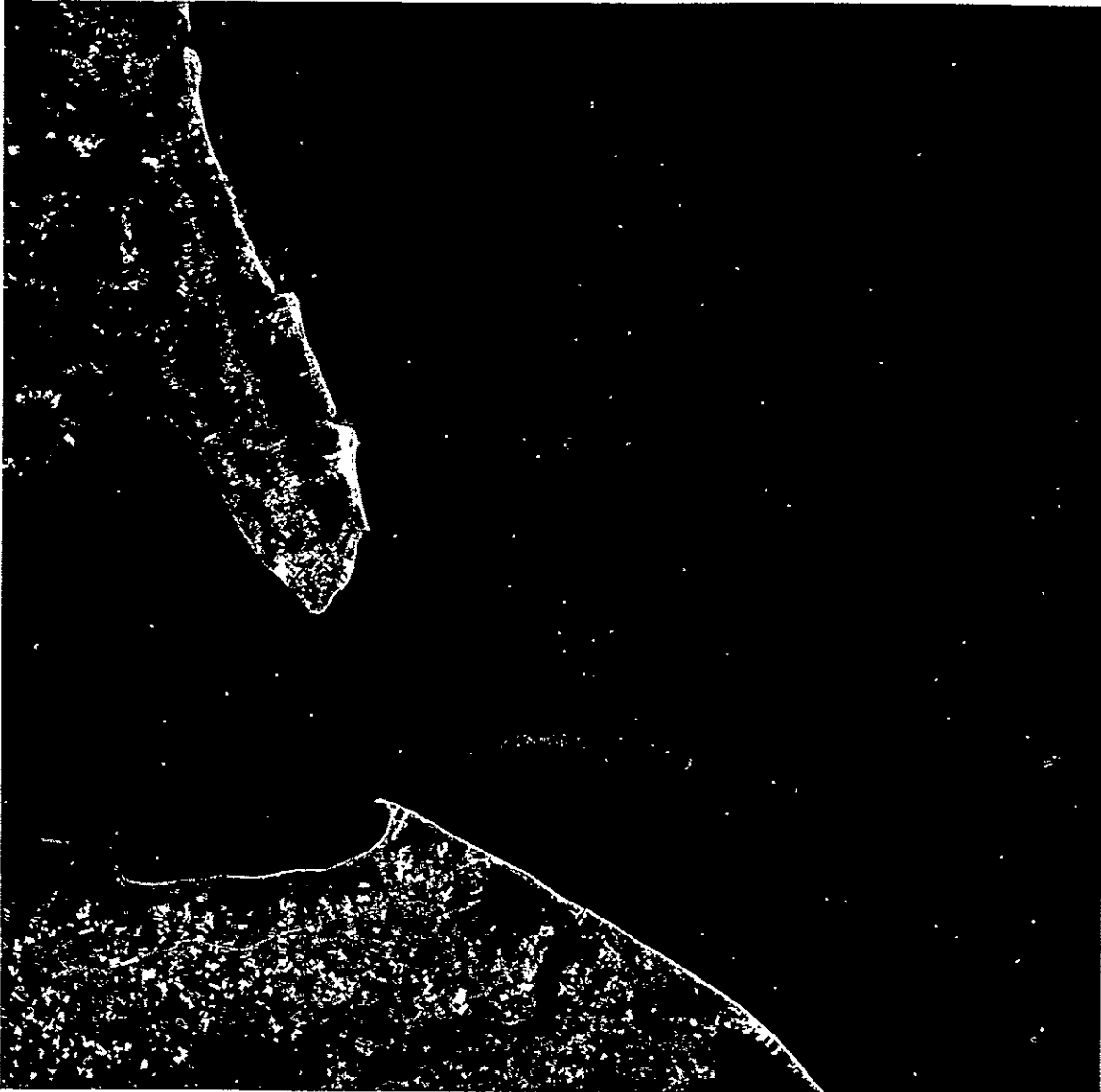


Figure 4.3 Skylab/EREP photograph of the Delaware Bay region obtained with the S190B earth terrain camera on September 12, 1973

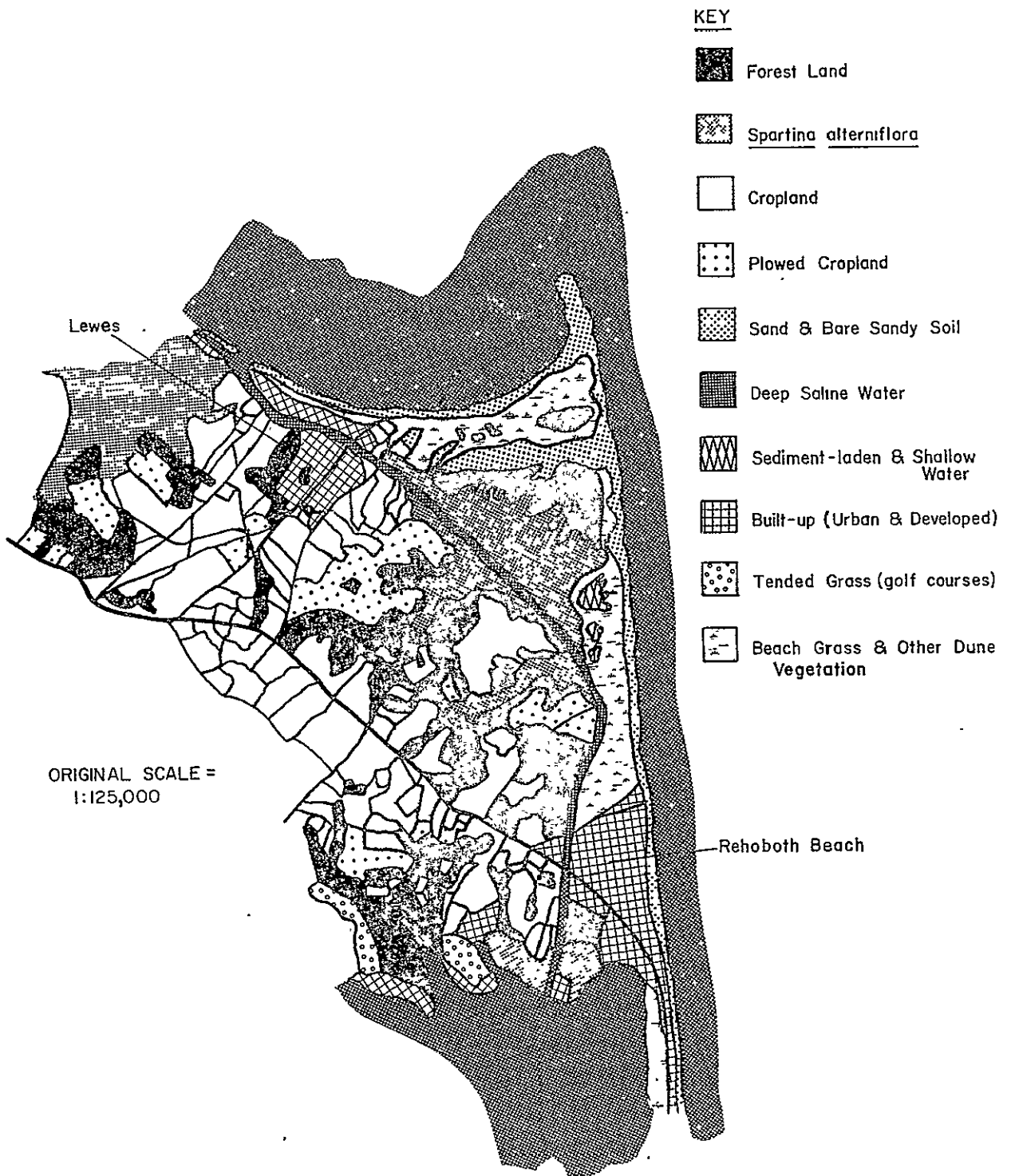


Figure 4.4 Land-use map derived from Skylab/EREP image by visual photo-interpretation

TABLE 4.2

Classification Accuracy Table Derived by Comparison of EREP-Interpreted,
Thematic Map of Figure 4.4, with USGS-CARETS Land Use Map

<u>Category</u>	<u>Forest</u>	<u>Wetland</u>	<u>Water</u>	<u>Agric.</u>	<u>Sand</u>	<u>Dune</u>	<u>Built-Up</u>
Forest	82%	3%	--	13%	<1%	--	3%
<u>S. alt.</u>	10%	88%	2%	--	--	--	<1%
Water	--	<1%	98%	<1%	<1%	--	<1%
Agriculture	5%	<1%	<1%	81%	--	--	13%
Sand	--	--	6%	4%	85%	--	6%
Dune	14%	23%	--	10%	--	6%	47%
Built-Up	--	2%	<1%	14%	2	--	81%

ORIGINAL PAGE IS
OF POOR QUALITY

Accuracy analysis was performed by comparison of the EREP-derived thematic map (Figure 4.4) with a USGS-CARETS Land-Use Map compiled at a scale of 1:100,000 from aerial photography acquired in 1970. The date and classification scheme of this data was largely, but not completely, compatible with the EREP-derived map. The difference in date of data acquisition forced abandonment of the distinction between Planted and Plowed Cropland (EREP categories 3 and 4) which were combined into an "Agriculture" category. Differences in the categories identified eliminated the Tended Grass (EREP category 9) category from the analysis and required the combination of EREP categories 6 and 7 into a single "Water" category. Some problems were also encountered with identifying a CARETS equivalent to the Dune and Beach Grass EREP category (#10). It is believed that the CARETS maps are the most appropriate, objective alternate data source for analysis and that the comparison of the maps does indicate the relative accuracies of classification even though all the EREP categories could not be included.

A grid consisting of 1 mm squares was used to check the EREP interpretation, square by square, against the CARETS classification. The CARETS data was reduced to 1:125,000 on the available copies at which scale each grid square corresponded to an area on the ground of $\sim 16,625 \text{ m}^2$. 6687 grid squares were checked -- a total area on the ground of $\sim 104 \text{ km}^2$. The resulting classification accuracy table may be seen in Table 4.2.

The 98% accuracy of Water classification is not surprising in that water boundaries were used to register the two data sources for comparison. In general, the discrimination of water boundaries is not a difficult task and so the bias introduced through registration is not considered significant.

The wetlands plant Spartina alterniflora was correctly classified into the CARETS "Vegetated Wetlands" category in 88% of the cases examined. Most confusion occurred with adjacent Forest lands -- probably due to misregistration rather than spectral confusion. Comparison of the EREP map directly with larger scale aerial photography indicates that accuracy of S. alterniflora may be lower due to some inclusion of other wetland species in this category. The wetlands of the area are pre-dominantly S. alterniflora however, and so actual accuracy probably is not lower than 80%.

Sand was correctly mapped 85% of the time with roughly equal confusion occurring with Water, Agriculture, and Built-Up categories. Such apparently even distribution of errors among categories often found adjacent to sand is suggestive of misregistration of the comparison data sources rather than spectral non-differentiation.

Forest lands were identified with an accuracy of 82% with most confusion occurring with the Agricultural category. It is thought that this confusion is partially due to spectral confusion between light crown cover forests and certain crop types in the S190B color photograph used as the primary interpretation source.

Identification accuracy of Agriculture was 81% with most omissions occurring in Built-Up areas. It was observed through inspection that most of this confusion occurred in rural residential communities of low density for which the spatial resolution of EREP data was apparently insufficient to make identification. Likewise, most commission errors of the Built-Up category were in the Agricultural class -- a situation reflecting the similarity at small scales of low density residential communities and agricultural areas including access roads and a variety of farm buildings. Identification of building types is probably necessary for better discrimination of these categories, a task which in such cases is beyond the resolution limitations of EREP data.

The accuracy shown on Table 4.2 for the Dune category may not be completely representative of its true accuracy of classification. The extensive confusion with the Built-Up category is real and appears to be the result of spectral similarities with tree-lined residential streets. The composite reflectance of tree crowns, concrete streets and sidewalks and building roofs make such areas spectrally indistinct from sparse dune vegetation overlying highly reflective sand. The trees also tend to obscure the spatial cues (rectangular street patterns) which were used in visual identification of Built-Up areas. It is in the detection of street patterns that the spatial resolution of S190B is of primary importance, and this accounts for the quantitative advantage of visual interpretation over automated spectral analysis in the mapping of Built-Up areas (see Section 5.3). The significant commission errors encountered in misclassification of Dune areas as Forest, Wetland, and Agriculture are more difficult to interpret. The

CARETS designation does not include a "Dune" category as such but rather subsumes such areas in the "Sand other than beaches" class. Inspection of the CARETS map indicates substantial errors in the identification of this class, often misclassifying it as "Bare rock" (a category not to be found in this coastal area) and "Light crown cover forest" which includes the shrubby transitional zones between sandy areas and forest or wetlands. Thus, the identification of Dunes is probably much better in the EREP map than in CARETS data. As with S. alterniflora, direct comparison of the EREP map with aerial photography was performed and indicated no significant confusion of Dune areas with any category other than Built-Up. Thus, the true accuracy for the Dune category would be approximately 50%.

A word is needed concerning the problem of registering two data sources preparatory to accuracy analysis such as was performed for this study. The investigator is forced to tread a fine line between achieving accurate registration and the biasing of results by use of the identified categories as a means of registration, thereby forcing equivalence of the data sources in those areas and categories used for registration. For this study, water boundaries were used for registration as they are to be found in many places within the scene and also because biasing of water identification is less critical than would be the biasing of other categories for which identification is more difficult. The use of only one type of feature as a means of registration, however, undoubtedly reduces the accuracy of registration. Add to this the usual problems in registration of two maps compiled at different scales by different interpreters and the result is apparent misclassifications which are actually produced by misregistration. Such "false" errors may account for a significant percentage of the total errors for any of the non-water categories and so the figures in Table 4.2 are conservative estimates to the extent that misregistration has occurred.

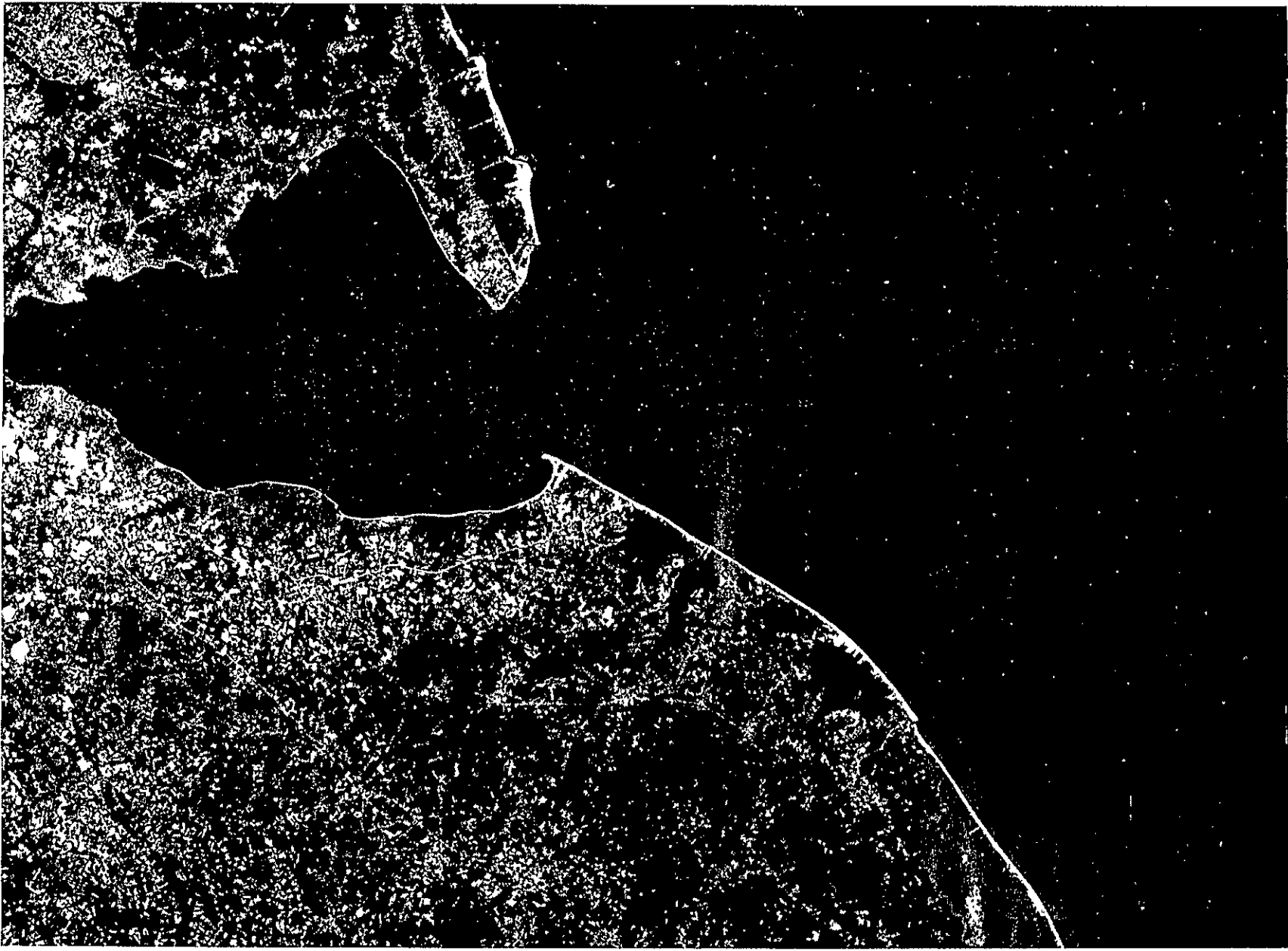


Figure 4.5 Photograph of Delaware Bay region obtained by Skylab/EREP S190A multispectral photographic facility on September 12, 1973 in the "Green" band (0.5-0.6 microns). (Scale = 1:344,000)

4.2 Coastal Processes and Water Properties

Figures 4.5, 4.6, and 4.7 contain photographs of the Delaware Bay region obtained with the Skylab/EREP multispectral photographic facility in the bands 0.5-0.6 microns, 0.6-0.7 microns, and 0.8-0.9 microns, respectively. Maps interpreting the major water features photographed by the Skylab/EREP pass on September 12, 1973, are shown in Figures 4.8 and 4.9. These two figures correspond to the S190A and S190B images, respectively. The coverage of Figure 4.1, of course, is identical to that of Figures 4.2, 4.5, 4.6, and 4.7. The water properties discerned in Figures 4.8 and 4.9 include suspended sediment patterns, river effluents, general surface current circulation, ocean waste dump plumes, tidal inundation of wetlands, water-land boundaries, and ship traffic.

4.2.1 Suspended Sediment Patterns and Current Circulation

Based on previous experience gained from the analysis of LANDSAT imagery,^{2,14} suspended sediment visible in Figures 4.5 and 4.3 was used as a natural tracer to permit photo-interpreters not only to deduce the behavior of individual river effluents, but also to study the overall bay and coastal current circulation patterns. The tidal current conditions in the Skylab S190A 0.5-0.6 micron band picture of Figure 4.5 are shown in Figure 4.10. Maximum ebb currents exist at the mouth of the bay; there is a low water slack upstream at the triple-bend near the C & D Canal; and flood currents prevail north of the C & D Canal (Delaware City). The suspended sediment patterns inside the bay show flow lines which agree with the expected current directions given in Figure 4.10. Strong sediment concentrations are visible over shallow areas, particularly shoals on the Cape May side of the bay mouth. This is caused by heavier particles being brought into short-term suspension by waves and rapid currents over the shoals. Suspended sediment plumes are also clearly emanating from the inlets and bays along the Atlantic coast of Delaware and New Jersey. The direction of these plumes indicates that at the time of this overpass, along the New Jersey coast, e.g., at Wildwood, the near-shore current was toward the north, while along Delaware's coast, e.g., at Indian River Inlet, the near-shore current was in the southerly direction.

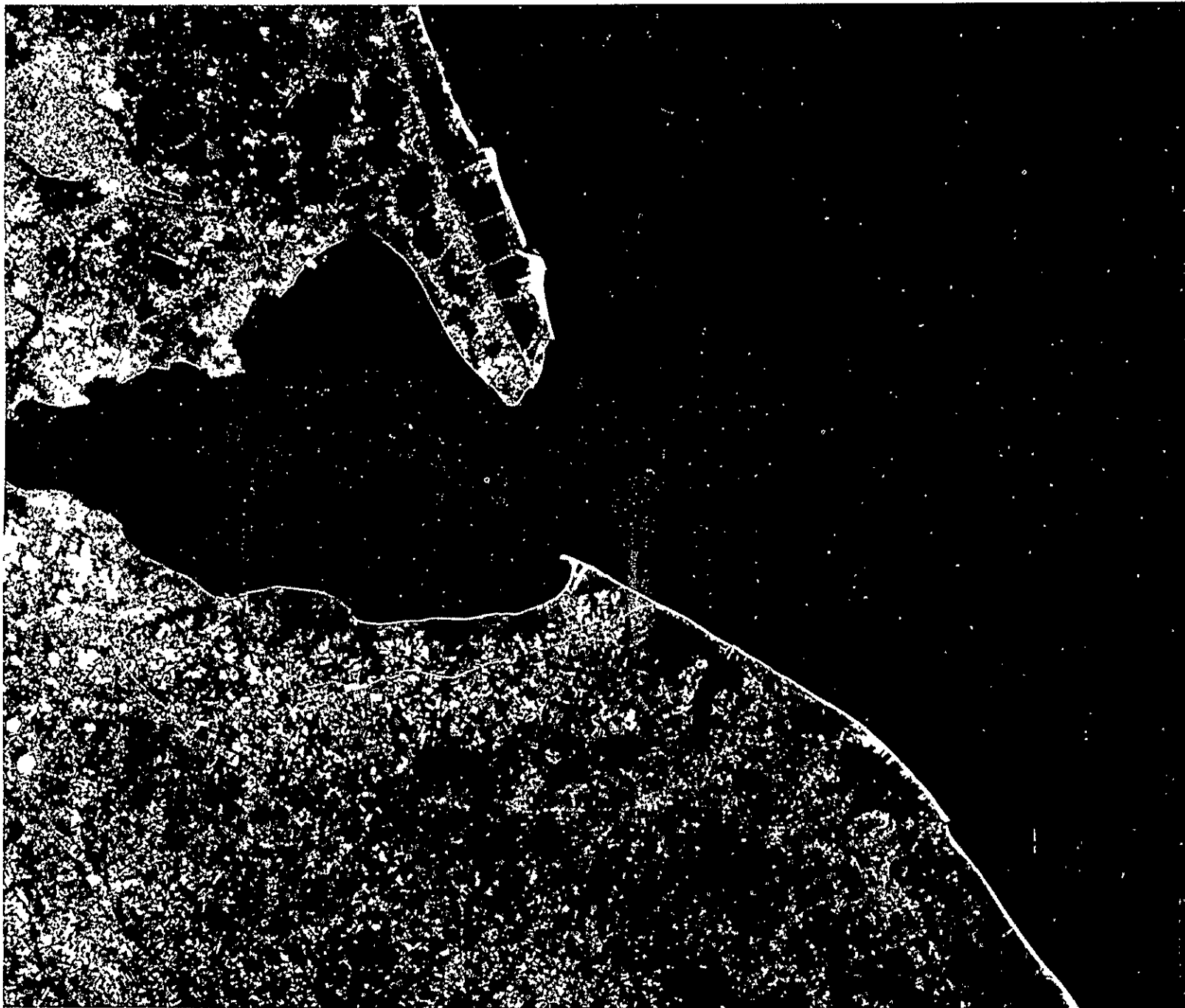


Figure 4.6 Photograph of Delaware Bay region obtained by Skylab/EREP S190A multispectral photographic facility on September 12, 1973 in the "red" band (0.6-0.7 microns). (Scale = 1:344,000)

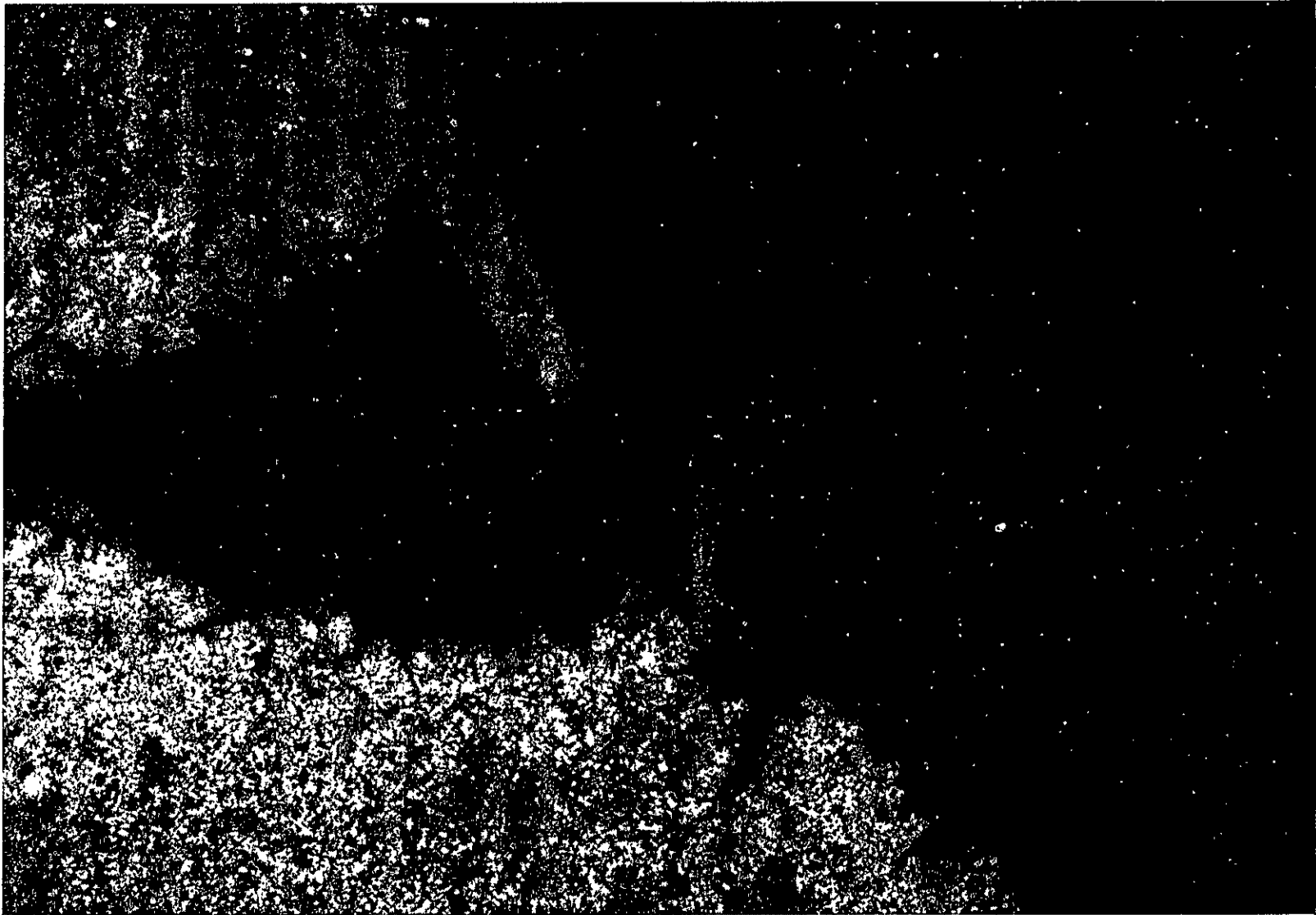


Figure 4.7 Photograph of Delaware Bay region obtained by Skylab/EREP S190A multispectral photographic facility on September 12, 1973 in the near-infrared band (0.8-0.9 microns). (Scale = 1:344,000)

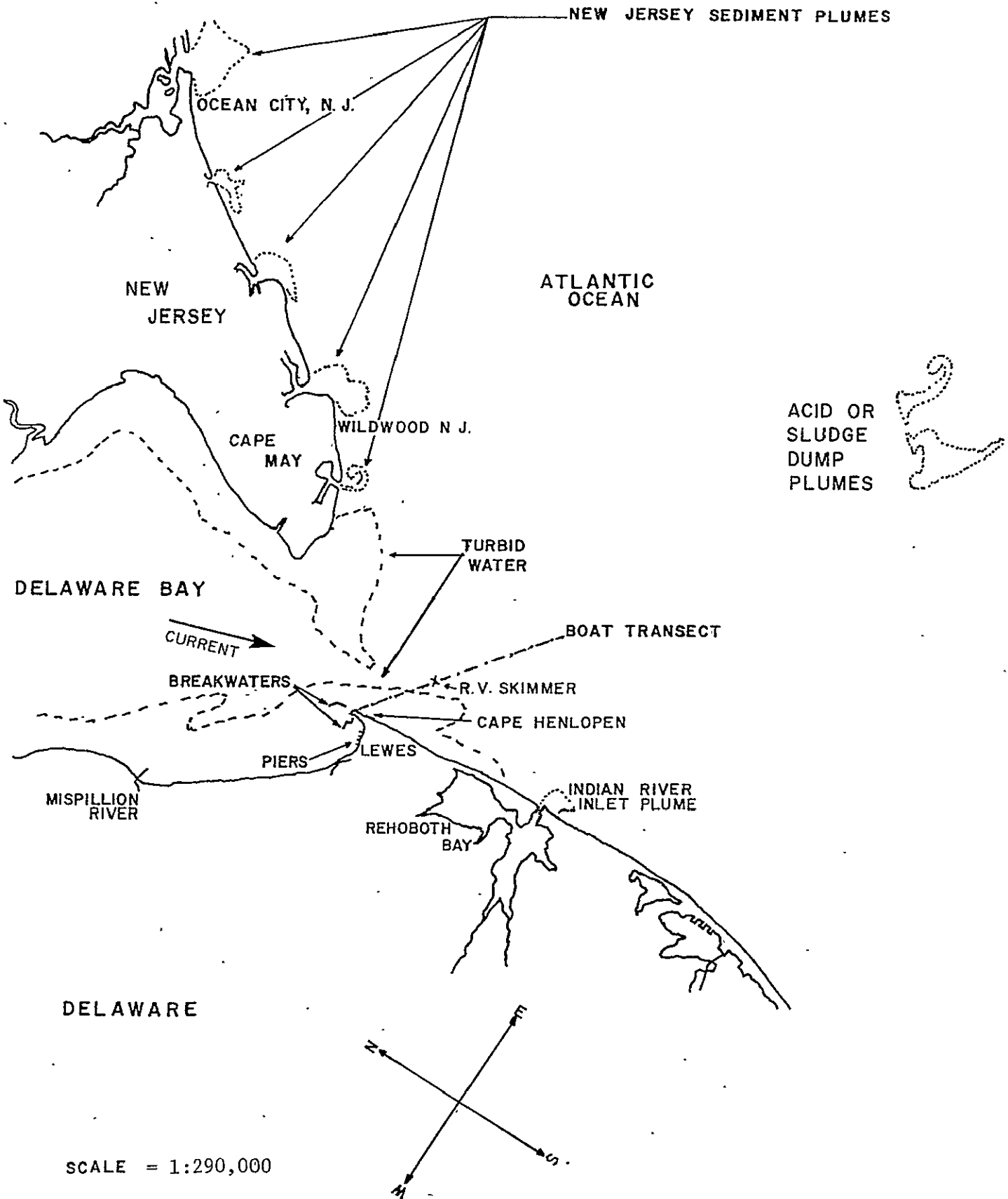


Figure 4.8 Interpretative map of major water features visible in Skylab/EREP S190B photograph shown in Figure 4.3 (Track 43, Rev. 1747, September 12, 1973).

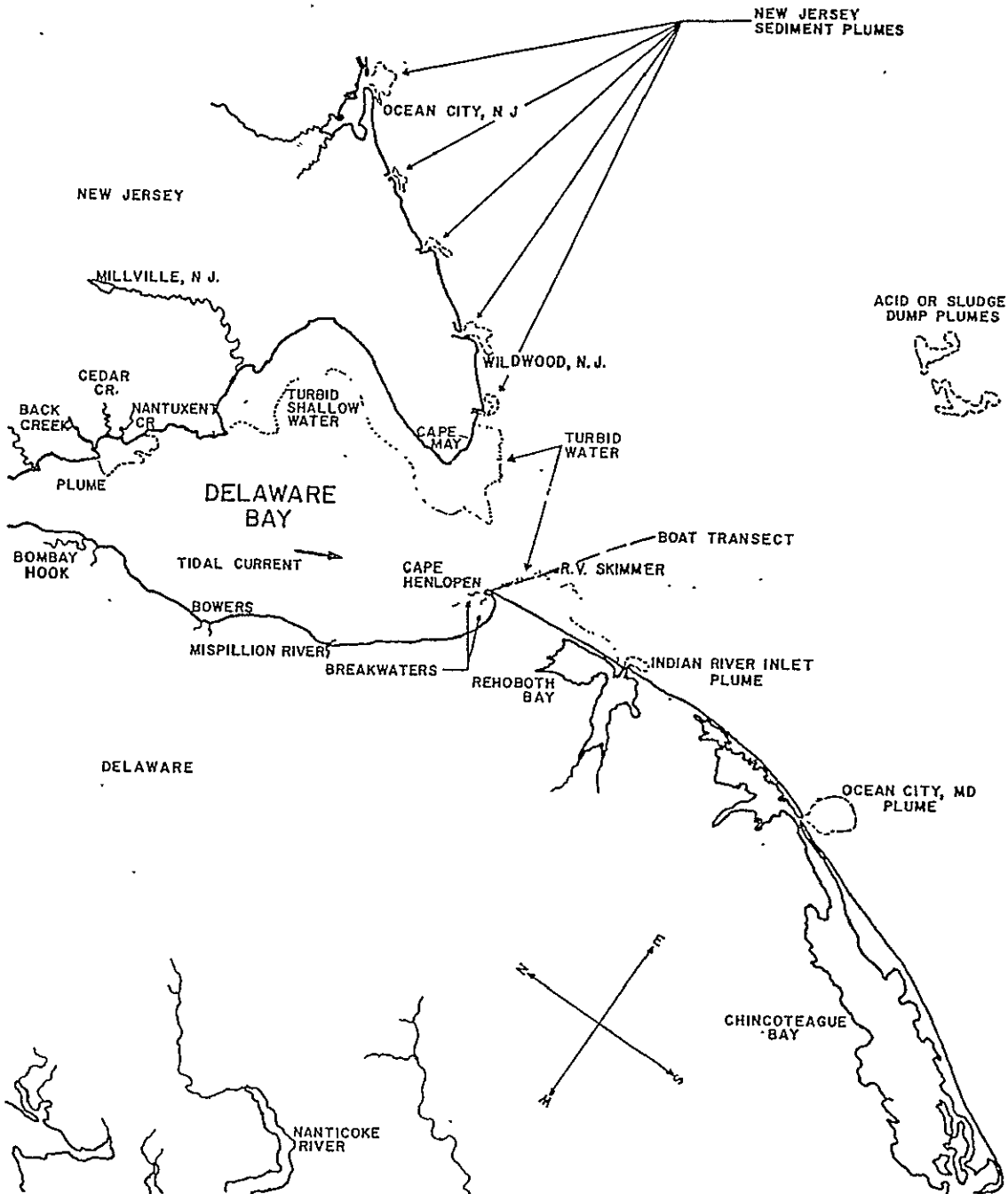


Figure 4.9 Interpretative map of major water features visible in Skylab/EREP S190A photograph shown in Figure 4.5. (Track 43, Rev. 1747, September 12, 1973) (Scale = 1:344,000).

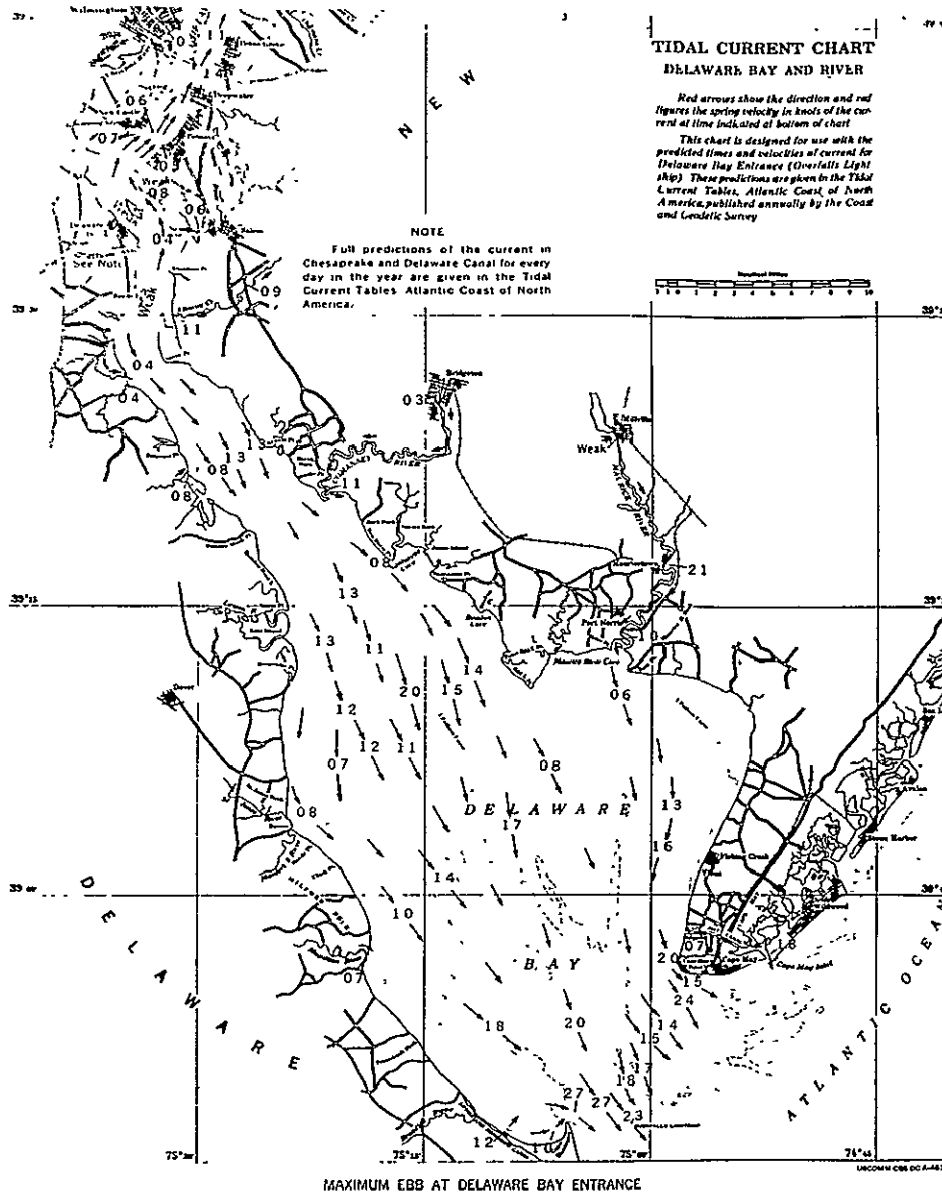


Figure 4.10 Approximate tidal current conditions in Delaware Bay during the Skylab/EREP overpass on September 12, 1973 (maximum ebb at Delaware Bay entrance)

ORIGINAL PAGE IS
OF POOR QUALITY

One water sampling transect was made on the day of the Skylab overpass, as shown in Figure 4.8. Along the transect the sediment concentration ranged from 30 to 50 mg/l, the water temperature from 21.4° to 22.8°C, and the salinity from 29.0% to 30.3%. Since the boat transect was made several hours after the Skylab overpass, and the sediment patterns are known to change in that area within a half hour's time, no attempt was made to correlate Skylab image radiance with suspended sediment concentration. However, color density slicing of the S190A 0.5-0.6 micron band photograph shown in Figure 4.5 provided a well defined distribution pattern of suspended sediment in the upper few meters of the water column.

Because the water samples collected after the Skylab overpass were not suitable for quantitative interpretation of the Skylab photographs, it was decided at least to compare the water features visible in Skylab photographs with those identified in LANDSAT imagery. The tidal current conditions in the Skylab picture of Figure 4.5 are similar to those in the LANDSAT image of Figure 4.11. This means that the Skylab pass over Delaware Bay on September 12, 1975, occurred during the same portion of the tidal cycle as the LANDSAT pass on May 13, 1973. Note the striking similarity between suspended sediment patterns in those two figures. The discussion of suspended sediment and current circulation patterns in the previous paragraphs based on the Skylab picture in Figure 4.5 directly applies to the LANDSAT image shown in Figure 4.11. The Skylab picture orientation differs from that of LANDSAT mainly because Skylab orbits have an inclination of 50 degrees, whereas those of LANDSAT are nearly polar.

It is also interesting to compare the tidal situation in the Skylab image of Figure 4.5 with LANDSAT images taken one hour after (Figure 4.12) and one hour before (Figure 4.13) the tidal condition represented in the Skylab image. In addition to LANDSAT imagery, Figures 4.12 and 4.13 contain tidal current maps of Delaware Bay (U. S. Department of Commerce, 1960). Each LANDSAT picture is matched to the nearest predicted tidal current map within ± 30 min (U. S. Department of Commerce, 1972). The current charts indicate the hourly directions by arrows and the velocities of the tidal currents in knots. The Coast and Geodetic Survey made observations of the current from the surface to a maximum depth of 6 m

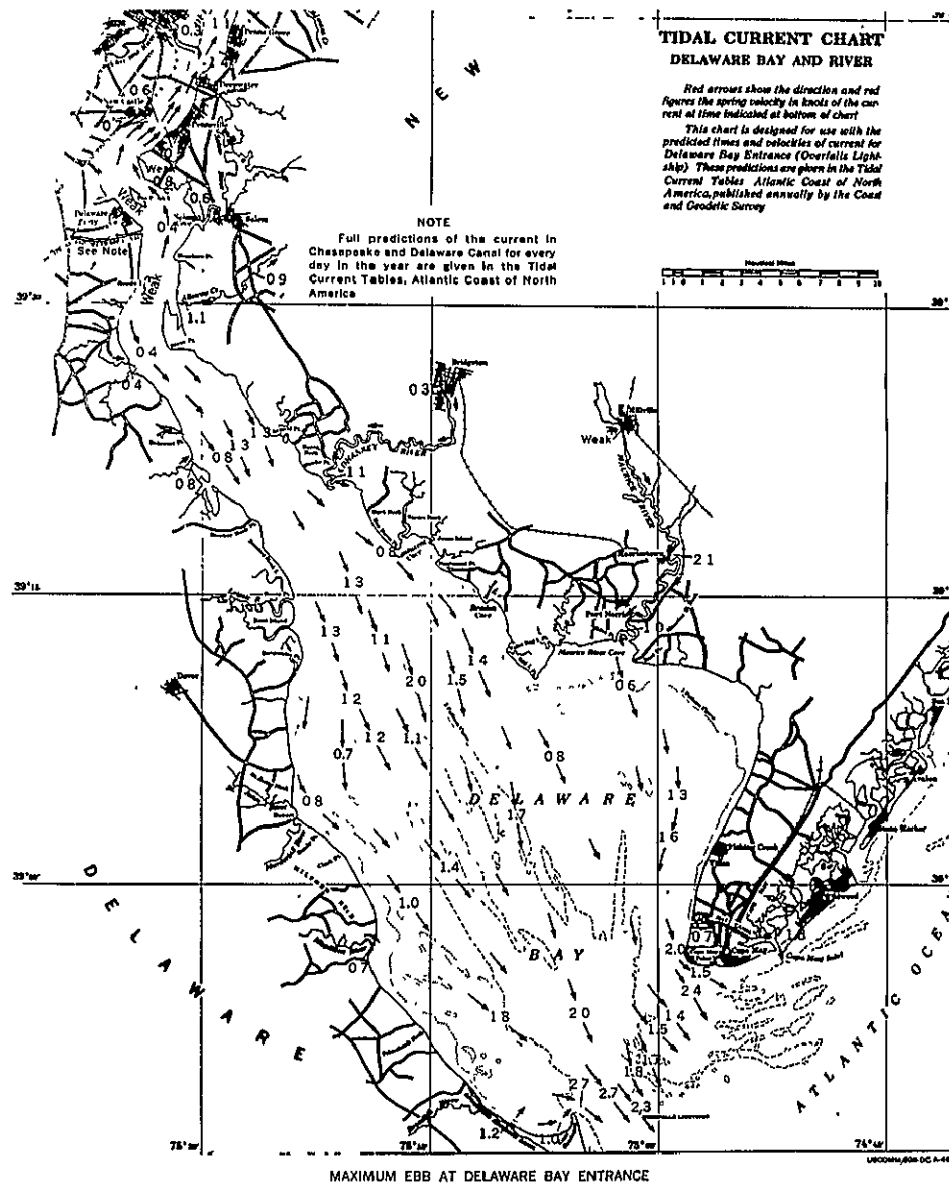


Figure 4.11 Predicted tidal currents and LANDSAT MSS band 5 image of Delaware Bay taken on May 13, 1973 (maximum ebb at Delaware Bay entrance)

in compiling these charts (U. S. Department of Commerce, 1960).¹¹ The LANDSAT overpass on February 13, 1973 occurred about one hour after maximum ebb at the mouth of the bay. The corresponding LANDSAT image and predicted tidal currents are shown in Figure 4.12. Strong sediment transport out of the bay in the upper portion of the water column is clearly visible, with some of the plumes extending up to 30 km out of the bay.¹² Small sediment plumes along New Jersey's coast indicate that the direction of the near-shore current during the overpass was still toward the north. The wind velocity at the time of the satellite overpass was about 13 km per hour from the north-northwest, reinforcing the tidal current movement out of the bay.

On the other hand, one hour before maximum ebb, as shown in Figure 4.13, the plumes from the coastal inlets and out of the bay were still weak and in the process of being formed. Low water slack was occurring in the upper portion of the bay, with small river plumes visible downstream and upstream from Bombay Hook and the Cohansey River. The wind was steady from the west at 13 to 16 km per hour.

During LANDSAT overpasses, ground truth was collected from boats and helicopters along transects across the bay, including measurements of Secchi depth, suspended sediment concentration, transmissivity, temperature, salinity, and water color. NASA aircraft flights over the Delaware Bay region performed in support of LANDSAT and Skylab programs included four overflights by the C-130, and three by the U-2. However none of these aircraft flights occurred during Skylab overpasses.

As shown in Figure 4.15, LANDSAT image radiance of bands was correlated with water sample analysis to produce maps of suspended-sediment concentration in the upper one meter of the bay. MSS band 5 seemed to give the best representation of sediment load in the upper one meter of the water column. Color density slicing helped delineate the suspended sediment patterns more clearly and to differentiate turbidity levels. Density slicing of all four LANDSAT bands gave an indication to relative sediment concentration as a function of depth, since the four bands penetrate to different depths ranging from several meters to several centimeters, respectively. Similar results would be expected if color density slicing of all S190A bands had been performed.

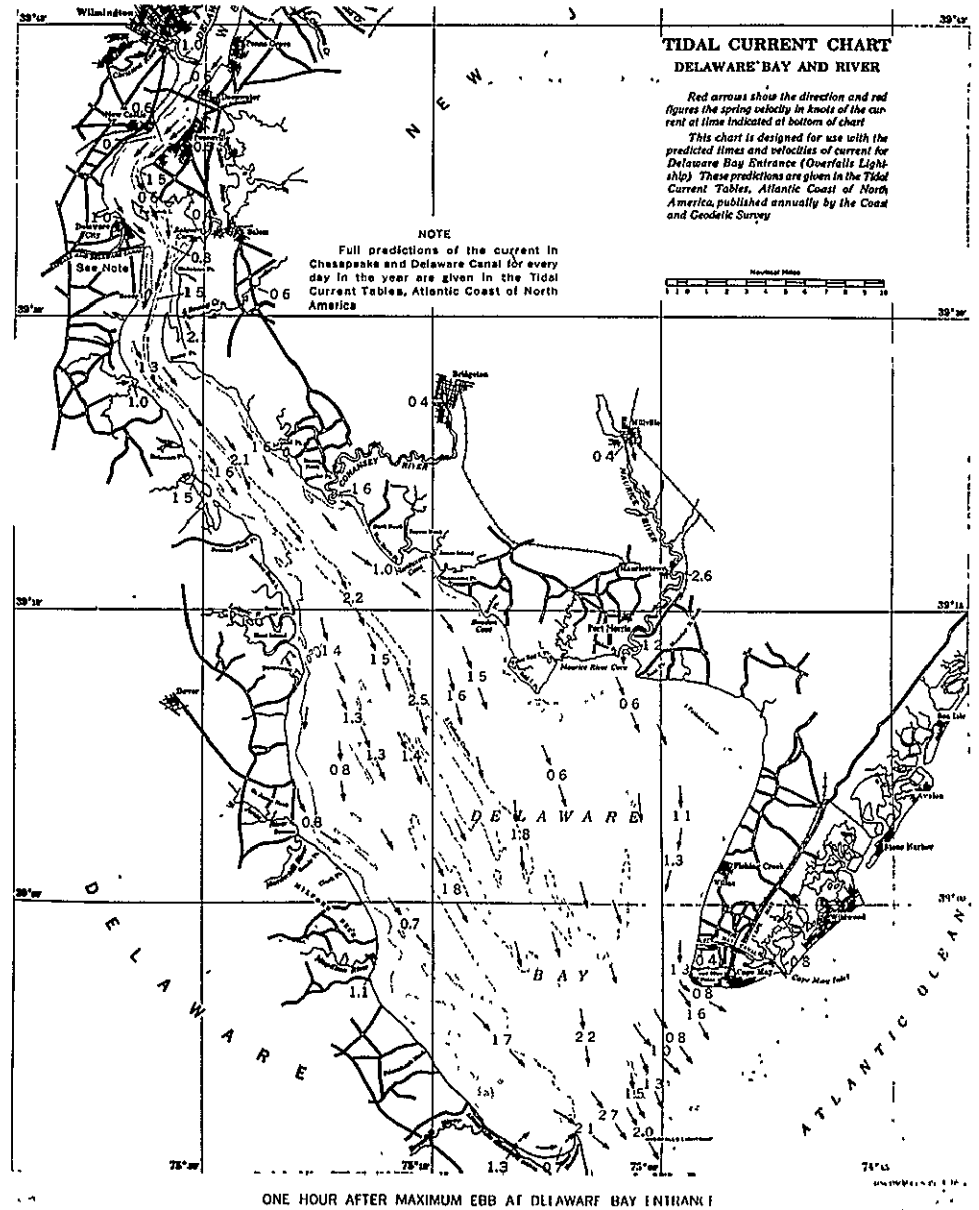
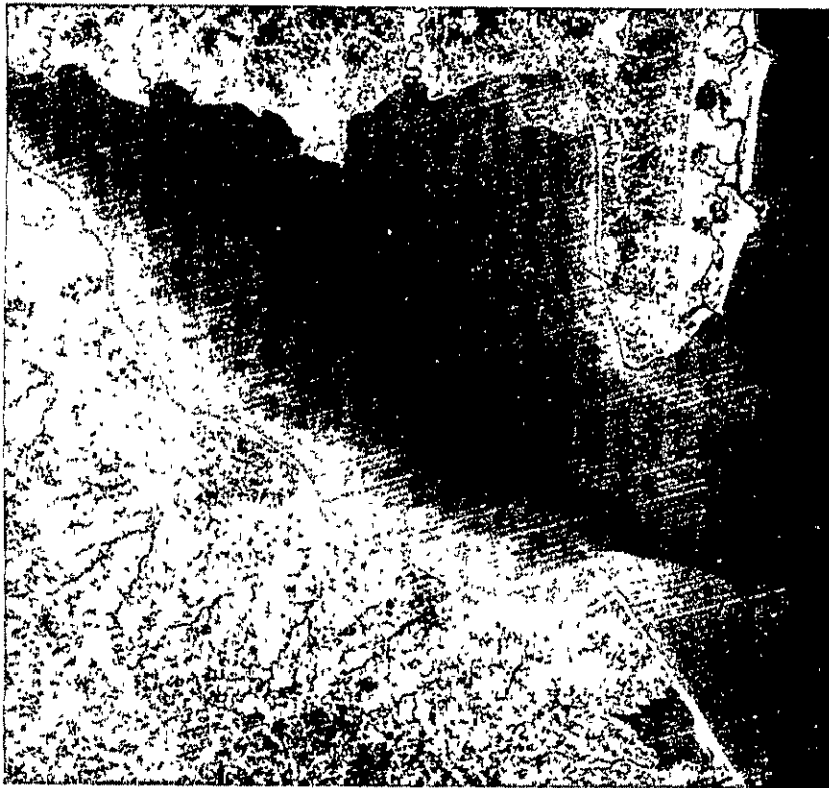


Figure 4.12 Predicted tidal currents and LANDSAT MSS band 5 image of Delaware Bay taken on February 13, 1973 (I.D. No. 1205-15141)

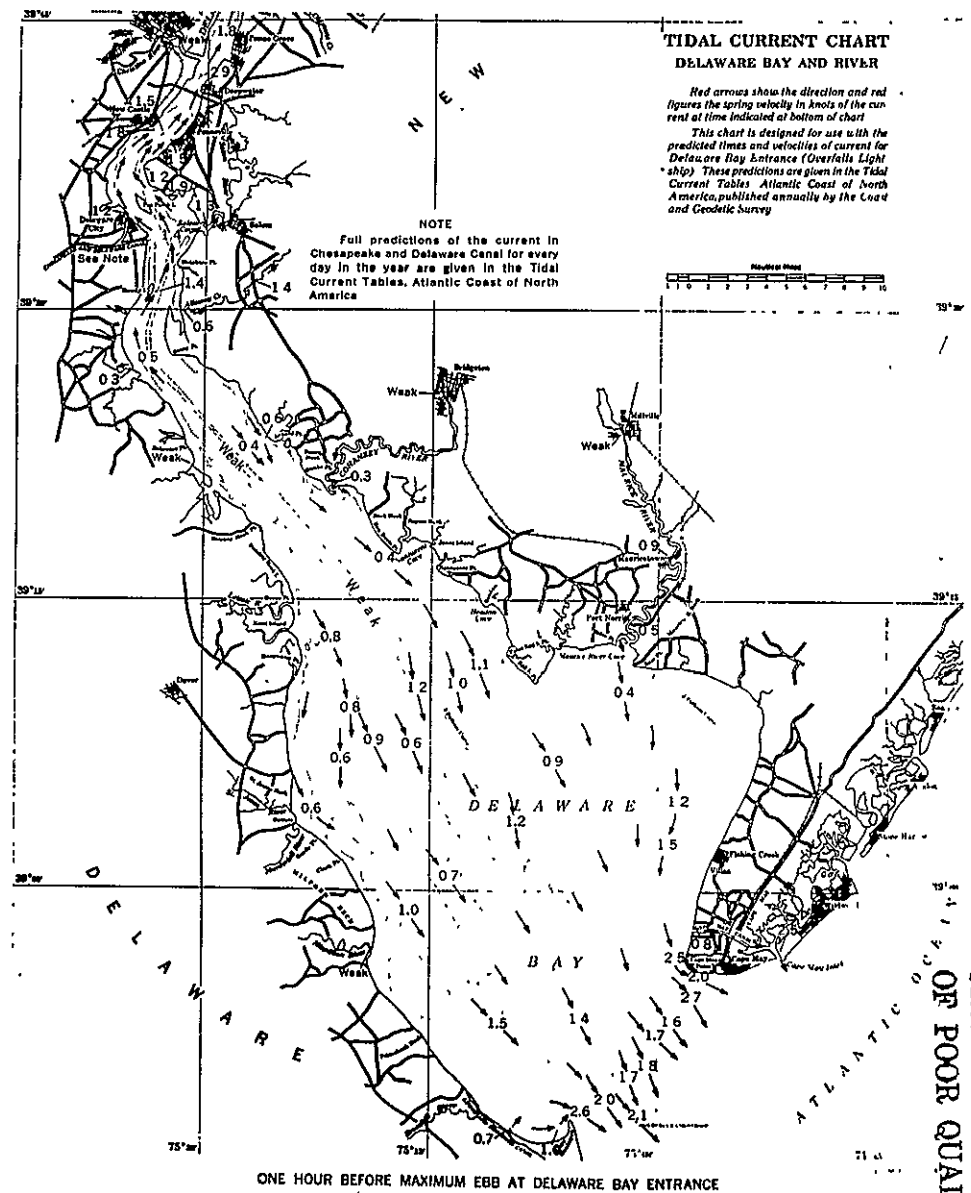
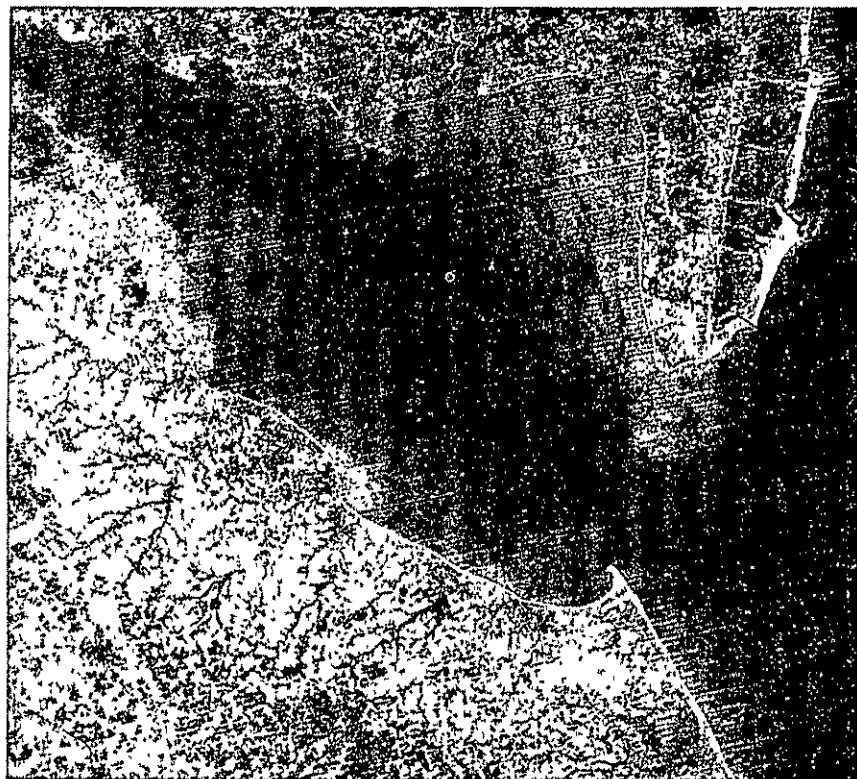
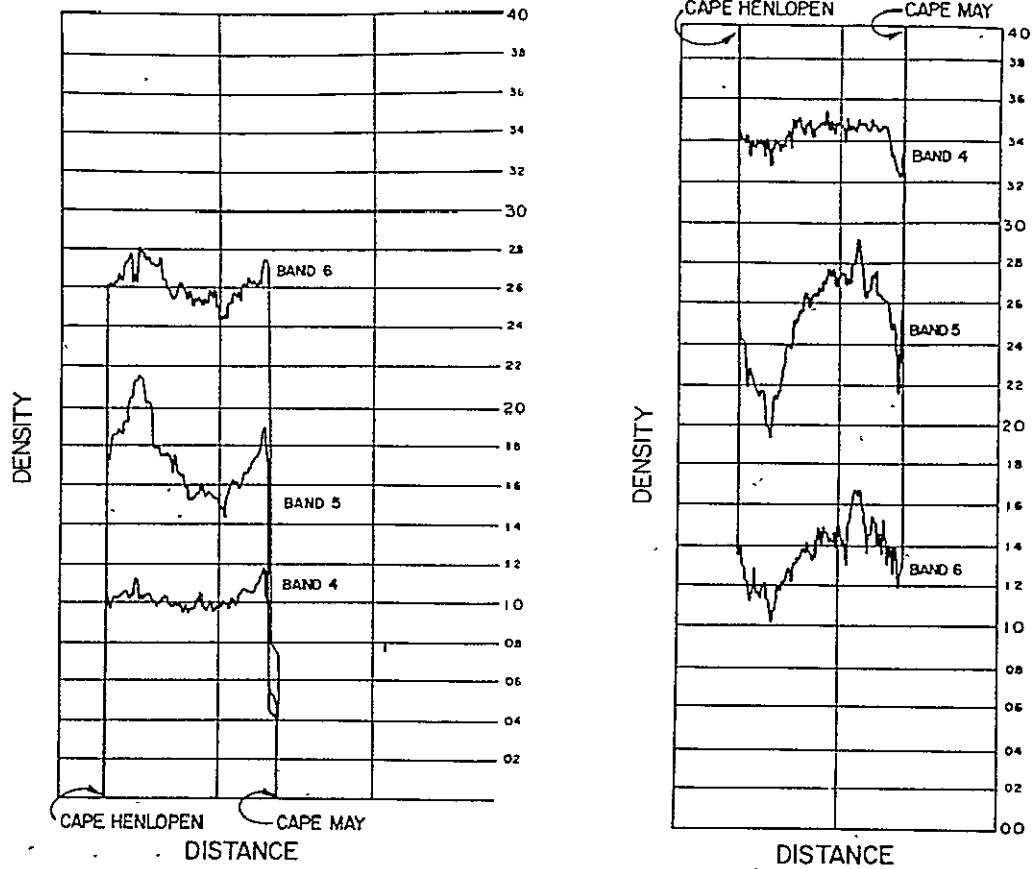


Figure 4.13 Predicted tidal currents and LANDSAT MSS band 5 image of Delaware Bay taken on December 3, 1972 (one hour before maximum ebb at Delaware Bay entrance)



a) Positive transparencies

b) Negative transparencies

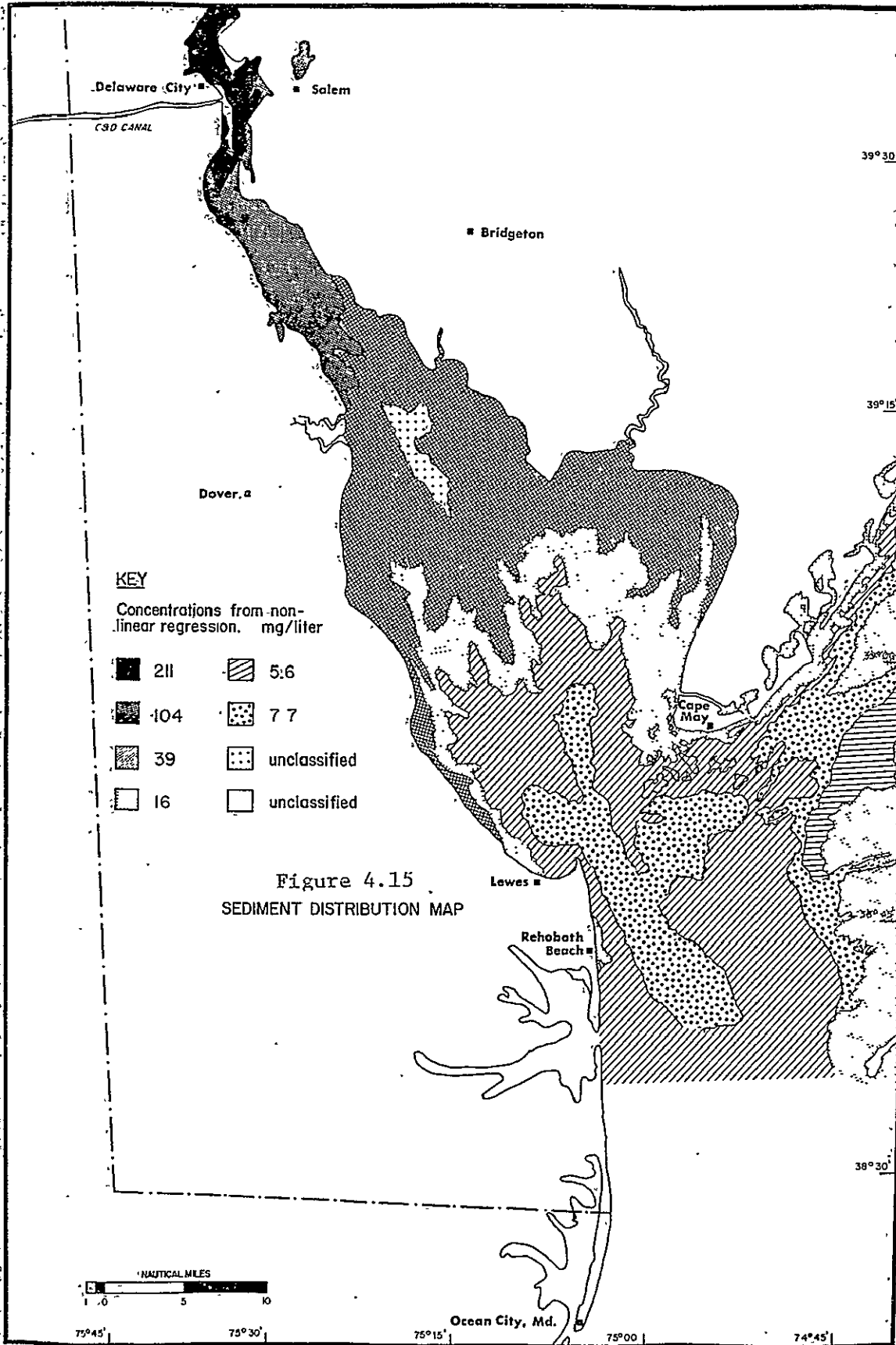
Figure 4.14 Microdensitometer traces of October 10, 1972, LANDSAT image from Cape Henlopen, Delaware, to Cape May, New Jersey, using MSS bands 4, 5, and 6.

Another notable feature in Skylab photographs of Figure 4.5, are boundaries or frontal systems inside the bay and along the coast. Those appear to be the same as studied in previous LANDSAT programs.^{2,14} Boundaries or fronts (regions of high horizontal density gradient with associated horizontal convergence) are a major hydrographic feature in Delaware Bay and in other estuaries. Fronts such as the ones shown in Figure 4.5 have been investigated in LANDSAT programs using STD sections, dye drops and aerial photography. Horizontal salinity gradients of 4‰ in one meter and convergence velocities of the order of 0.1 m/sec have been observed. Underwater visibility improved from one meter to two meters as certain boundaries were crossed. Several varieties of fronts have been seen. Those near the mouth of the bay are associated with the tidal intrusion of shelf water. The formation of fronts in the interior of the bay appears to be associated with velocity shears induced by differences in bottom topography with horizontal density difference across the front influenced by vertical density difference in the deepwater portion of the estuary. Surface slicks and foam collected at frontal convergence zones near boundaries were found to contain concentrations of Cr, Cu, Fe, Hg, Pb, and Zn higher by two to four orders of magnitude than concentrations in mean ocean water.¹³

By capturing and holding oil slicks, frontal systems such as the ones shown in Figure 4.5 significantly influence the dynamic behavior of oil slicks in Delaware Bay. Recent oil slick tracking experiments conducted by the authors in order to verify a predictive oil dispersion and movement model have shown that during certain parts of the tidal cycle the oil slicks tend to line up along boundaries.¹⁵ Therefore the predictive model may have to be modified to include information on boundaries and frontal systems. Combining spacecraft imagery with air-tracked drogues and ships proved to be a most effective means of assessing the performance of the oil slick movement and dispersion model.

4.2.2 Spatial Resolution and Ship Traffic Monitoring

It is well known that one can detect bright or long narrow objects having widths well below the resolution limit of the sensor, if they



contrast strongly against their background.¹⁶ This explains our ability to discern our ground truth boat, canals, highways, and the breakwaters near Cape Henlopen, all having widths narrower than predicted Skylab resolution limits. On the other hand, resolution is based on the photographic criterion of image quality as related to the observable minimum spacing of bar targets of specified design.¹⁶

Comparing Figures 4.3 with Figures 4.10 and 4.12, one discerns more detail in the Skylab/EREP photographs than in the LANDSAT images. Only the Skylab S190B picture can distinguish the piers near Cape Henlopen, shown in Figure 4.3. The detailed structure of flow patterns and sediment plumes is also more clearly visible in the Skylab photographs. The difference becomes particularly apparent if one compares the sediment plumes at Indian River Inlet, Delaware; Ocean City, Maryland; and along the New Jersey coast. Both breakwaters and the location of our boat are visible in the Skylab photograph. The ability to discern ships of various sizes directly or by their wakes throughout the Delaware Bay region makes Skylab an attractive platform for ship traffic observation in congested coastal water, especially if repetitive coverage were to become available.

Comparing the S190A "green" band shown in 4.5 with the "red" LANDSAT band (band 5) image in 4.11 the difference in spatial resolution becomes small, especially if carefully reconstructed images from ERTS-1 digital tapes are used. For instance, the two breakwaters inside Cape Henlopen can be clearly discerned in Skylab photographs and in LANDSAT images which were reconstructed by the Bendix Aerospace Division from 9-track magnetic tapes.¹⁴ The same breakwaters cannot be distinguished in the "quick-look" 70mm bulk black and white transparencies obtained from NASA directly.

Therefore, in comparison to the 20-40 m resolution attributed to the S190A Multispectral Photographic Facility, the LANDSAT multispectral scanner appears to have a resolution of about 70-100 m. These results are in agreement with predicted resolution figures.^{17,18}

4.2.3 Observation of Ocean Waste Disposal Plumes

Thirty-eight nautical miles southeast of Cape Henlopen, Delaware is located the disposal site for waste discharged from a plant processing

ORIGINAL PAGE IS
OF POOR QUALITY



Figure 4.16 Enlarged digital enhancement of acid waste plume imaged
by LANDSAT on January 25, 1973

titanium dioxide. The discharge is a greenish-brown liquid containing 17% to 23% acid (expressed as H_2SO_4) and 4% to 10% ferrous sulfate. The barge which transports this waste is capable of releasing one million gallons of the liquid upon radio-command from a towing tug. It makes at least four trips to the disposal site per month.

Careful examination of the Skylab/EREP images in Figures 4.5, 4.3 and 4.1 reveals two waste plumes about 30 to 40 miles east off the Delaware-Maryland coast. One of the plumes seems to represent acid wastes dumped 32 hours before the overpass, while the second plume is either part of the same dump or remnants from a dump 65 hours before overpass. The greenish-grey color of the plume makes it most visible in the 0.5-0.6 micron band shown in Figure 4.5, followed by the color photo of Figures 4.3 and 4.1, encompassing the entire visible spectral region. The red band shown in Figure 4.6 which was effective for suspended sediment mapping is not as useful anymore. Enlarged enhancements of the acid waste patterns aided considerably in studies of the distribution of the wastes.

The frequency of the dumping made it possible for the LANDSAT satellite to image the waste plume in various stages of degradation, ranging from minutes to days after dump initiation. Fourteen images were found which show water discoloration in the general vicinity of the waste dump site. The spectral characteristics and position of the discoloration, the dump pattern and the time difference between the dump and photograph gave strong indications that the discolorations are the acid waste plume.

As an example, careful examination of the image of January 25, 1973, discloses a fishhook-shaped plume about 40 miles southeast of Cape Henlopen caused by a barge disposing acid wastes. Figure 4.16 shows an enlarged enhancement of the acid waste pattern, prepared from LANDSAT MSS digital tapes which aided considerably in studies of the dispersion of the wastes. Digital radiometric print-outs of the waste plumes are presently being correlated with concentrations of dissolved and particulate substances, such as iron, sampled from boats at the time of aircraft and satellite overpasses. The change in concentration over cross sections of the plume are used to determine dispersion properties

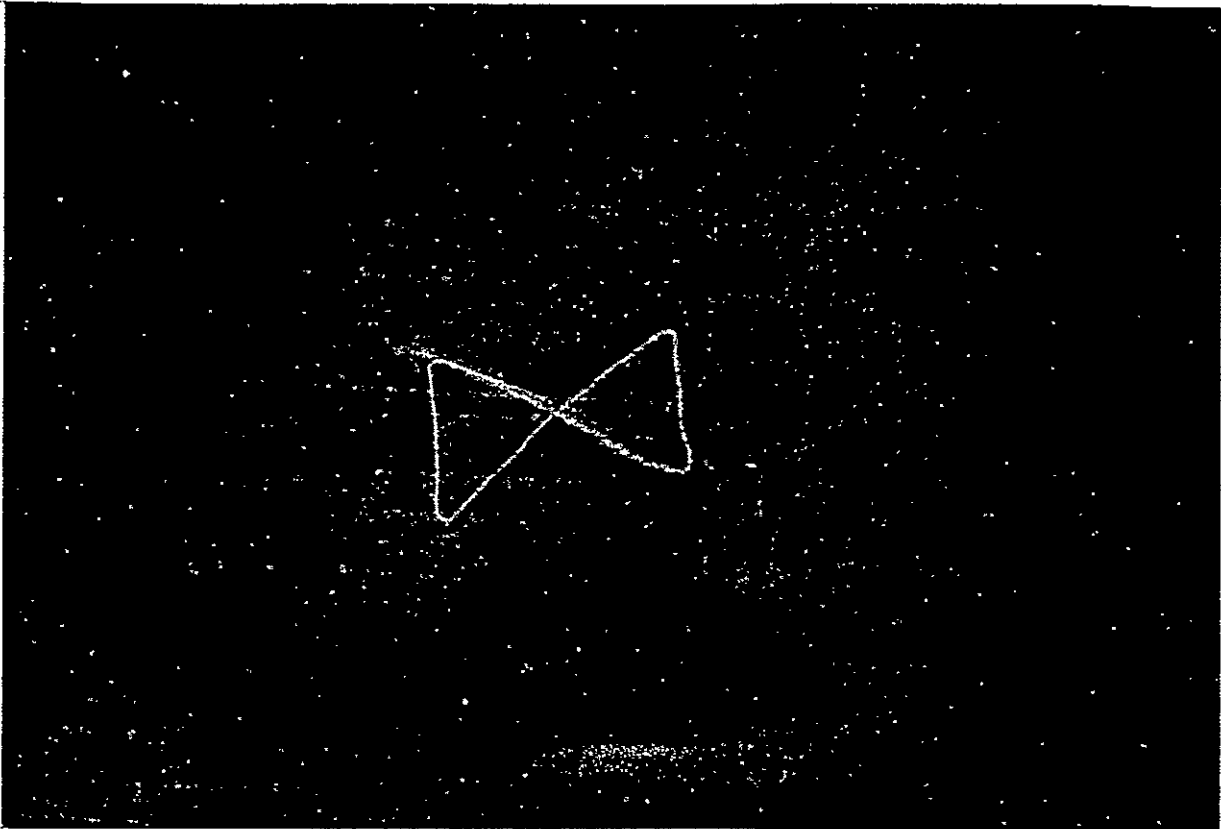


Figure 4.17 Enlarged LANDSAT MSS band 4 picture of barge dumping acid wastes at DuPont Company's ocean waste dump site

of the waste. Spectrometers deployed from helicopters and boats have also been used to determine spectral signatures of waste plumes such as the one in Figure 4.17, imaged by LANDSAT on August 28, 1975, having the new figure-eight dump configuration. Spectrometric measurements indicate that, upon combining with seawater, the acid waste develops a strong reflectance peak in the 0.55 to 0.60 micron region, resulting in a stronger contrast in the LANDSAT MSS band 4 than the other bands.

It is unfortunate that the acid waste plumes photographed by the S190A and S190B cameras are not contained in the S192 multispectral scanner imagery. As shown in Figure 3.1, the swath width of the S192 was considerably narrower than that of the film cameras and missed the acid plumes altogether. As a result it was not possible to conduct an analysis of the spectral signature of the acid plumes using the thirteen multispectral scanner bands.

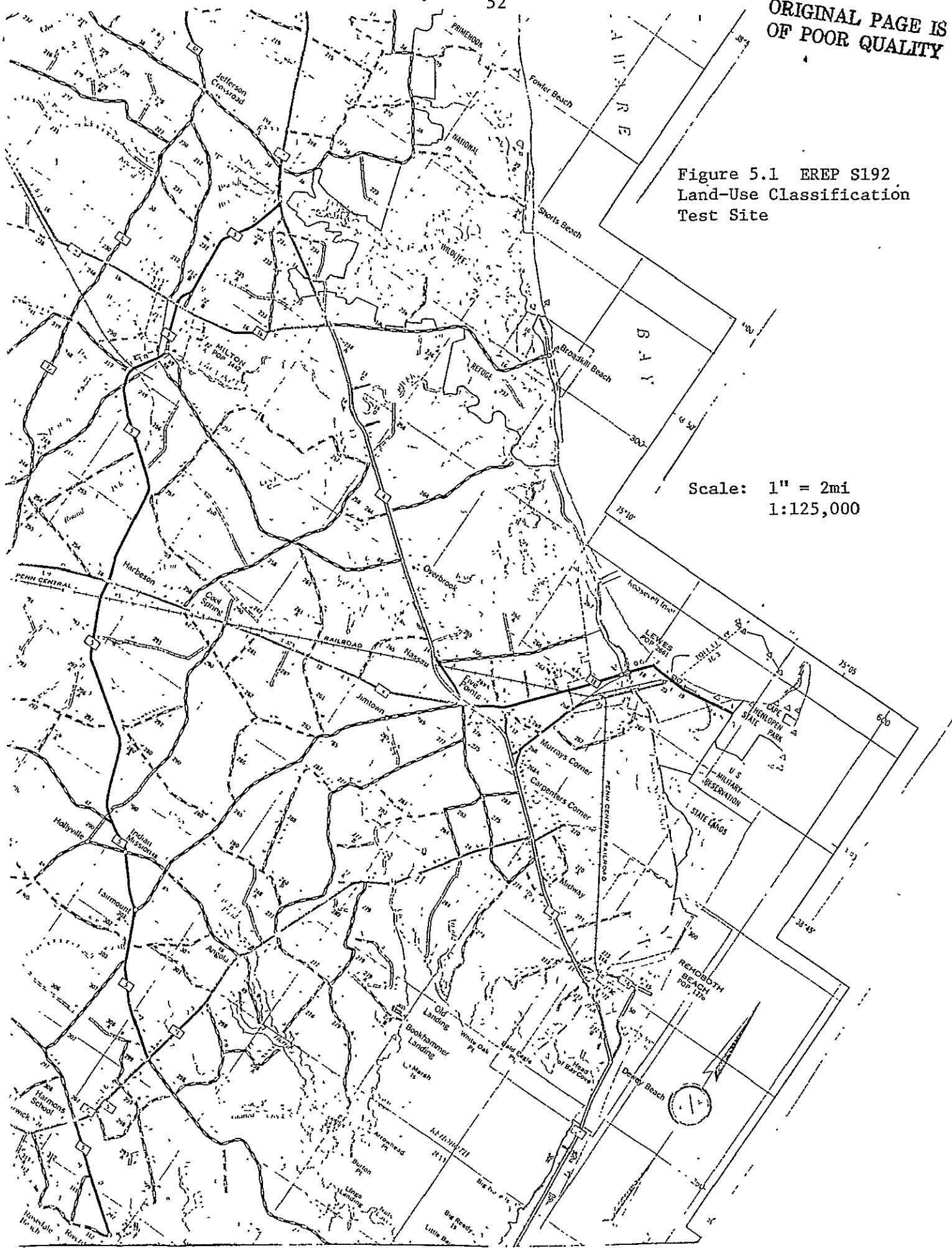


Figure 5.1 EREP S192
Land-Use Classification
Test Site

Scale: 1" = 2mi
1:125,000

5.0 S192 MULTISPECTRAL SCANNER RESULTS

5.1 Test Site

The test site chosen for automated multispectral analysis encompasses the entire width of the S192 scanner swath extending from the Indian River-Rehoboth Bay complex in the south to Slaughter Beach in the north (Figure 5.1). East-west (along orbital path) boundaries were chosen to include the coastal area of Delaware and extend some miles out into Delaware Bay and the Atlantic Ocean (Figures 5.1 and 3.1). It is unfortunate from an operational point of view that the entire state of Delaware was not covered; however, the test site described does encompass the following area: an extremely active ship channel at the mouth of Delaware Bay; part of the Atlantic shelf; coastal environments of the Delaware Bay; part of the Atlantic shore and barrier beach-lagoon system; the towns of Lewes and Rehoboth Beach, Delaware; three large tidal marsh systems and large areas of most other characteristic Delaware land uses. In addition, the Lewes area has been proposed as a major staging center for Outer Continental Shelf development facilities; therefore, land-use mapping and environmental baseline studies of the region are of great interest to the state and local planners.

5.2 Analysis Procedure

5.2.1 Screening of Raw Data

Noise-filtered and linearized S192 scanner data became available in late 1975 and has been screened and analyzed. Band 3 (.52-.52 μ) was not present in noise-filtered data (although it was on the original, unfiltered tapes) but all other S192 bands were examined. Screening of bands was accomplished on a Bendix multispectral analysis system with computer-refreshed visual display.¹⁹ Data from each band was examined alone and in combination with others and the resulting single-band density slices and false color composites were visually compared with NASA-RB57 aerial photographic ground truth.

Band 1 (.41-.46 μ) was very poor in quality. Heavy banding and possibly haze-induced noise obscured most of the spatial and spectral detail. Band 2 (.46-.51 μ) was of considerably better quality although

over water, where this wavelength band could find best use, sufficient noise was present to mask most structure visible in S190 photographs of the same area. Band 3, as mentioned previously, was not present. Band 4 (.56-.61 μ) was of good quality and was chosen for tests of multispectral classification. Band 5 was also found to be of good quality although features in water were not clearly discriminated. Band 6 was chosen for use in testing multispectral classification. Bands 7 (.78-.88 μ), 8 (.98-1.08 μ), 9 (1.09-1.19 μ) and 10 (1.2-1.3 μ) were all found to be of good quality, and band 8 was chosen for multispectral classification. Band 11 quality was excellent and it also was chosen for use in multispectral classification. Band 12 (2.1-2.35 μ) and the thermal channel, band 13 (10.2-12 μ) were noisy and could not be used.

In general, the quality of data appeared good and had been significantly improved by noise filtering. Some sync drop-outs were still evident, however, and banding and noise in low-signal areas (i.e., water) obscured much of the structural detail observed in the EREP photographic experiments. For this reason, no spectral classification within water was performed. Atmospheric effects apparently degraded band 1, while thermal-IR measurements (band 13) during the daylight overpass showed little promise of utility.

Multispectral classification was accomplished using a General Electric Image 100 analysis system. The system uses an operator-controlled cursor and visual display for rapid acquisition of training data. The classification algorithm chooses the high and low value in each band, edited from any given training set, to derive a four-dimensional radiance window. A window is thus derived for each training set (category) and new data classified using these windows. This high speed algorithm allows rapid production of enhanced results but is somewhat limited in accuracy by comparison with more complex probabilistic algorithms such as "maximum likelihood."

Image 100 uses up to five bands at a time for enhancement analysis but one channel is utilized for storage if a multi-category classification is performed. Thus, four bands may be used in combination, in four-dimensional analysis.

The four bands utilized (4-.56 to .61 μ , 6-.68 to .76 μ , 8-.98-1.08 μ ,

and 11-1.55-1.75 μ) were chosen for (1) expectation of good classification results on land, based on original screening and comparison with ground truth; (2) approximate correlation with the LANDSAT-MSS bands: 4 (.5-.6 μ), 5 (.6-.7 μ) and 7 (.8-1.1 μ) to provide continuity of results obtained from the two systems; and (3) band 11 was chosen because other workers have suggested that extending analysis further into the reflective infrared can produce good results in land-use mapping.¹⁸

The Image 100 system can accommodate an eight-category classification scheme.

5.3 Results of Multispectral Classification

The eight-category scheme chosen for the test site is as follows:

<u>Category No.</u>	
1	Forest
2	<u>Spartina alterniflora</u> (Salt Marsh Cord Grass)
3	Water
4	Plowed Fields
5	Cropland (Planted)
6	Sand and Bare Sandy Soil
7	Built-Up Land
8	<u>Typha</u> sp. and <u>Phragmites communis</u> (Cattails and Giant Reed Grass)

The Image 100 classification of each category was performed. Accuracy analysis similar to that performed on the imagery-derived land-use map (Section 4.1.1) was used to generate the figures shown in Table 5.1. A 1 mm grid was again used to quantify the comparison between the S192-derived category maps and an alternate data source -- the USGS-CARETS land-use map. Differences in classification systems and dates of acquisition required that category 8 (Typha sp. and Phragmites communis) be eliminated from the analysis and that categories 6 and 7 (Plowed Fields and Cropland) be combined into a single Agriculture category. A Bausch and Lomb "Zoom Transfer Scope" was used to overlay optically and register the category maps with the CARETS base,

and a test area consisting of 5000 grid squares ($\sim 78 \text{ km}^2$ on the ground at 1:125,000 scale) was compared, square by square. Some problems with registration were encountered as the computer-generated category plots are not geometrically corrected and the anamorphic correction capability of the Zoom Transfer Scope was used to offset this distortion.

TABLE 5.1

Classification Accuracy Table Derived by Comparison of S192-Derived Thematic Plots of Figures 5.2-5.9 with USGS-CARETS Land-Use Map

<u>Category</u>	<u>Forest</u>	<u>S.alt.</u>	<u>Water</u>	<u>Agri- culture</u>	<u>Sand</u>	<u>Built- Up</u>
Forest	79%	10%	<1%	7%	0%	4%
<u>S. alt.</u>	12%	76%	<1%	5%	0%	7%
Water	0%	<1%	100%	0%	0%	0%
Agriculture	15%	3%	<1%	54%	8%	20%
Sand & Bare Sandy Soil	0%	<1%	<1%	17%	79%	3%
Built-Up	8%	<1%	3%	39%	6%	44%

Accuracy of identification for water is good (100%) as might be expected for the comparatively easy discrimination of water from terrestrial cover types. This figure may be slightly inflated, however, since water boundaries were used to register the two maps for comparison and some bias was undoubtedly encountered since this registration was based on the assumption that the water boundaries were correctly located. Past experience has shown that discrimination of water boundaries may be reliably performed when reflective infrared measurements are included in the analysis and so the bias introduced is not thought to be severe. All other categories were registered with respect to the water classification map and so no registration bias was encountered in their analysis.

Category number 6 (Sand and Bare Sandy Soil) was identified with 79% accuracy. Most commission errors indicated were with the Agriculture category (17%). Non-quantitative comparison of the category map with photographic coverage of the area indicated that almost all of the commission errors were located in an unplanted field of sandy soil. Since category 6 also includes "sandy soil" (CARETS mapped this into the Agriculture category) its true accuracy is above 90%.

S. alterniflora is the dominant tidal wetlands plant in Delaware and its presence is a reliable indicator of at least daily tidal inundation. Two major marshes were identified consisting almost entirely of this species while a third wetland area, less frequently flooded and dominated by other plants was properly omitted. Particularly important is the identification of small fringing marshes around Rehoboth Bay in the southeastern portion of the test site. Such fringes are important in shore stabilization and natural pollutant treatment but their presence had not previously been indicated in orbital data. Accuracy of identification was limited to 76%, primarily by confusion with Forested and Built-Up areas adjacent to the tidal wetlands.

Seventy-nine percent accuracy was achieved for Forest Land with confusion occurring in adjacent wetland and agricultural cover types. The commission errors encountered in both the S. alterniflora and Forest Land categories appear to be occurring with adjacent cover types and so misregistration of the comparison sources may be responsible for some of the apparent misclassifications.

Severe errors of commission in identification of Built-Up Land are indicated by the accuracy analysis, with most confusion occurring with Agriculture. In general, accuracy must be improved if spectral classification of Built-Up Land is to be of any use. The visual identification of Built-Up Land (see Section 4.1.1) relied heavily on the spatial arrangement of streets and thus the multispectral analysis is severely handicapped in inventorying this particular category.

The two cropland categories -- 4 (Plowed Fields) and 5 (Cropland) -- clearly dominate the region, totaling roughly 42% of the land area according to data generated by the EREP classification. Monitoring of agriculture in Delaware is not a high priority endeavor, although identification of agricultural uses in general would be necessary for detection of land-use change; in particular, removal of land from agricultural use for development purposes. Classification appears poor with major confusion occurring within the Built-Up category. Again, the use of spatial cues in visual interpretation (see Section 4.1.1) allowed much better discrimination of these categories than was possible using purely spectral analysis.

Category 8 (Typha sp. and Phragmites communis), although not included in quantitative accuracy analysis, appears visually to have encountered the most significant commission misclassifications of any of the categories. Most confusion occurs with other wetland species in the large marshes and with low areas of trees and shrubs to the west of Rehoboth Bay. Examination of category 8 signature histograms indicates a very similar signature to that of S. alterniflora, except in band 8 where separation is evident. A probabilistic classification algorithm may discriminate the two categories; although it is suspected that the training sets selected for Typha Phragmites have included other cover types. The category 8 signature is most similar to that for Forest Land, an unexpected phenomenon which points to inadvertent inclusion of trees in the training set selected for Typha Phragmites.

In general, accuracy analysis shows mixed results for automated multispectral analysis of S192 data. The somewhat ambitious classification scheme employed appears to have exceeded restrictions imposed by limited

spatial resolution -- particularly in the identification of human impacts (Built-Up Land and Agriculture). Furthermore, since available software allowed the simultaneous use of only four S192 bands, advantages to be derived from EREP's large number of spectral bands were minimized. A further restriction was the use of a non-probabilistic, "window" type classification algorithm in analysis. The accuracies achieved therefore probably represent conservative approximations of potential EREP results, although limited spatial resolution will continue to present problems. While comparison with LANDSAT results is not conclusive due to differing mission and research objectives, it appears that comparable results could be achieved using S192 data.

6.0 SUMMARY AND CONCLUSIONS

On September 12, 1973, Skylab/EREP imaged the Delaware Bay test site under nearly cloud-free conditions. Skylab/EREP film products from the S190A Multispectral Photographic Facility and the S190B Earth Terrain Camera have been optically enhanced and visually interpreted to extract data suitable for:

- mapping coastal-land use
- inventorying wetlands plant species
- monitoring tidal conditions in estuaries
- observing suspended sediment patterns
- charting surface current circulation patterns
- separating water masses having different properties
- locating coastal fronts and boundaries
- monitoring industrial and municipal waste dumps in the ocean
- determining the location, size, and flow direction of river, bay and man-made discharge plumes
- observing ship traffic

The spatial resolution provided by Skylab photographic products makes possible small-scale land-use mapping, with a potential value of the final product to user groups such as state and local planning, conservation, and pollution-control agencies. Skylab film products were visually analyzed to identify and map ten land-use and vegetation categories at a scale of 1:125,000. Comparison of these thematic maps with CARETS Land-Use Maps resulted in classification accuracies ranging from 50% to 98%. Wetlands delineation in particular can benefit from inventory at such scales. The national wetlands inventory presently being planned by the Department of Interior, for example, anticipates the use of a 1:100,000 base-mapping scale.

Visual inspection of S190A and S190B film products gave a synoptic overview of suspended sediment patterns and ocean waste dump plumes at the mouth of Delaware Bay and on the continental shelf, respectively. Viewing the suspended sediment as a natural tracer it was possible to assess surface current direction from suspended sediment flow lines and

river plume shape and direction. Since ships generally represent bright, high-contrast targets against the dark ocean background, it was possible to detect them down to a long dimension size of about 15 meters and in many cases to examine their wake.

Digital tapes from the S192 Multispectral Scanner were used to prepare thematic maps of land use. Classification accuracies obtained by comparison of S192-derived thematic maps of land use with USGS-CARETS land-use maps in Southern Delaware produced accuracies ranging from 44% to 100%. The automatic classification achieved represents a conservative indication of S192 capabilities because of the somewhat unsophisticated classification algorithm used and the limited number of categories and band combinations available. Analysis of S192 data also suffered from reliance solely on spectral data, particularly in identification of built-up areas in which spatial cues are of value. S192 tapes were not analyzed for water features mainly because the noise level on the tapes made water feature identification and classification difficult, and because the S192 coverage frame did not include ocean waste dump plumes observed by the S190A and S190B cameras.

Based on the analysis of high-contrast pier structures and urban street line patterns, it appears that the S192 multispectral scanner has a resolution of about 70-100 m, the S190A Multispectral Photographic Facility about 20-40 m, and the S190B Earth Terrain Camera about 10-20 m.

7.0 RECOMMENDATIONS

1. Future manned spacecraft missions would be more beneficial if they could provide repetitive coverage of test sites. Two types of repeat cycles are important:
 - Seasonal, for land-use, vegetation inventory and environmental impact studies.
 - Hourly, for current circulation and pollution dispersion studies in tidal estuaries and coastal waters.
2. The conical scan in the S192 multispectral scanner should be replaced by a rectilinear scan because conical scanning makes direct readout more complicated and more expensive. Data should be delivered in rectilinear form regardless of the scan choice.
3. Orbits should be selected to minimize sun glint. This would help discriminate suspended sediments and pollutants in the water column.
4. A color infrared camera having a 5-inch or 9-inch format should be added or the color film in the S190B Earth Terrain Camera replaced by color infrared film. Color infrared film would be more effective for mapping land use and inventorying wetland vegetation if S190B resolution would be maintained.
5. A closer tie should be maintained between astronauts gathering the data from spacecraft and principal investigators who will analyze and use the data in order to optimize the value of the data returned.
6. More rapid data distribution should be established, particularly in the delivery of S192 tapes from NASA to principal investigators and data users.

8.0 REFERENCES

1. The Coastal Zone of Delaware, The Final Report of the Governor's Task Force on Marine and Coastal Affairs, College of Marine Studies Publication, University of Delaware, July 1972.
2. Klemas, V., Satellite Studies of Turbidity, Waste Disposal Plumes and Pollution-Concentrating Water Boundaries. Proceedings Second Conference on Environmental Quality Sensors, National Environmental Research Center, Las Vegas, Nevada, October 10, 1973.
3. Bopp, Frederick, III and Robert B. Biggs, Delaware Bay Report Series, Vol. 3, Trace Metal Geochemistry of Estuarine Sediments, Report No. 2, Trace Metal Environments Near Shell Banks in Delaware Bay, 45 pages, College of Marine Studies, University of Delaware, Spring 1973.
4. Oostdam, B. L., Suspended Sediment Transport in Delaware Bay, Ph.D. dissertation, University of Delaware, May 1971.
5. Ketchum, B. H., The Distribution of Salinity in the Estuary of the Delaware River, Woods Hole Oceanographic Institute, Ref. No. 52-103, 38 pages, 1952.
6. Harleman, D. R. F., Tidal Dynamics in Estuaries, Estuary and Coastline Hydrodynamics, A. T. Ippen, Ed., McGraw-Hill, New York, 1966.
7. Kraft, J. C., A Guide to the Geology of Delaware's Coastal Environment, College of Marine Studies Publication, University of Delaware, 1971.
8. Klemas, V., D. Bartlett, and R. Rogers, Skylab and ERTS-1 Investigations of Coastal Land Use and Water Properties, Proceedings AIAA/AGU Conference on Scientific Experiments of Skylab, Huntsville, Alabama, October 30-November 1, 1974.
9. Klemas, V., D. Bartlett, and R. Rogers, Coastal Zone Classification from Satellite Imagery. Photogrammetric Engineering and Remote Sensing, Journal of the American Society of Photogrammetry, Vol. 41, No. 3, April 1975.
10. U. S. Department of Commerce, Tidal Current Tables, Atlantic Coast of North America, National Oceanic and Atmospheric Administration, National Ocean Survey, 1972 and 1973.
11. U. S. Department of Commerce, Tidal Current Charts, Delaware Bay and River, Environmental Science Services Administration, Coast and Geodetic Survey, Second Edition, 1960.

12. Klemas, V., D. Bartlett, W. Philpot, and R. Rogers, Coastal and Estuarine Studies with ERTS-1 and Skylab, Remote Sensing of Environment, 3, 153-174, 1975.
13. Szekiolda, K.-H., S. Kupferman, V. Klemas, and D. F. Polis, Element Enrichment in Organic Films and Foam Associated with Aquatic Frontal Systems, J. Geophys. Res. 77, No. 27, September 20, 1972.
14. Klemas, V., M. Otley, W. Philpot, and R. Rogers, Correlation of Coastal Water Turbidity and Circulation with ERTS-1 and Skylab Imagery. Proceedings Ninth International Symposium on Remote Sensing of Environment, April 15-19, 1974, Ann Arbor, Michigan.
15. Klemas, V., G. Davis, and H. Wang, Remote Sensing of the Dynamic Properties of Coastal Waters and Pollutants, Proceedings of Symposium on Research Techniques in Coastal Environments. Louisiana State University, Baton Rouge, Louisiana, March 18-20, 1976. (Invited Paper)
16. Colvocoresses, A. P., Image Resolutions for ERTS, Skylab and Gemini/Apollo, Photogrammetric Engineering, No. 1, pp. 33-35, January 1972.
17. Slater, P. N., Multiband Cameras, Photogrammetric Engineering, No. 6, pp. 543-555, June 1972.
18. Bachofer, B. T., ERTS-1 Data Product Performance, Proceedings of Symposium on Significant Events Obtained from ERTS-1, NASA-GSFC, New Carrollton, Maryland, March 1973.
19. Bendix Aerospace Systems Division, M-DAS: Multispectral Data Analysis Systems, BSR 4146B, September 1974.

9.0 LIST OF RELATED PUBLICATIONS

1. Klemas, V., Detecting and Measuring Oil on Water. Instrumentation Technology, September, 1972.
2. Szekiolda, K.-H., S. L. Kupferman, V. Klemas, and D. F. Polis, Element Enrichment in Organic Films and Foam Associated with Aquatic Frontal Systems. Journal of Geophysical Research. Vol. 77, No. 27, September 20, 1972.
3. Kupferman, S. L., V. Klemas, D. F. Polis, and K.-H. Szekiolda, Dynamics of Aquatic Frontal Systems in Delaware Bay. A.G.U. Meeting, Washington, D.C., April 16-20, 1973.
4. Klemas, V., R. Srna, and W. Treasure, Assessment of Sediment Disposal Patterns on Delaware Bay by Use of ERTS-1 Satellite Imagery. Proceedings International Symposium on Interrelationships of Estuarine and Continental Shelf Sedimentation, Bordeaux, France, July 9-14, 1973.
5. Klemas, V., Requirements for Laser Systems Used in Coastal Investigation. Proceedings Conference on the Use of Lasers for Hydrographic Studies, Wallops Island, Virginia, September 12, 1973, Sponsors NASA, NOAA, EPA, NAVY (Invited Paper).
6. Klemas, V., J. F. Borchardt, and W. M. Treasure, Suspended Sediment Observations from ERTS-1. Remote Sensing of Environment, Vol. 2, 1973.
7. Klemas, V., R. Srna, W. Treasure, and R. Rogers, Satellite Studies of Suspended Matter and Aquatic Interfaces in Delaware Bay. Proceedings A.S.P. Symposium on Remote Sensing in Oceanography, Orlando, Florida, October 2-5, 1973.
8. Klemas, V., D. Bartlett, and F. Daiber, Mapping Delaware's Coastal Vegetation and Land Use from Aircraft and Satellites. Proceedings A.S.P. Symposium on Remote Sensing in Oceanography, Orlando, Florida, October 2-5, 1973.
9. Klemas, V., Satellite Studies of Turbidity, Waste Disposal Plumes and Pollution-Concentrating Water Boundaries. Proceedings Second Conference on Environmental Quality Sensors, National Environmental Research Center, Las Vegas, Nevada, October 10, 1973 (Sponsor EPA). (Invited Paper)
10. Klemas, V., D. Bartlett, R. Rogers, and L. Leed, Inventories of Delaware's Coastal Vegetation and Land Use Utilizing Digital Processing of ERTS-1 Imagery. Proceedings NAS Third ERTS-1 Symposium, Washington, D.C., December 10, 1973.

11. Klemas, V., M. Otley, G. Davis, and R. Rogers, Mapping Coastal Water Properties and Current Circulation with Spacecraft. Second Joint Conference on Sensing of Environmental Pollutants, Washington, D.C., December 10-12, 1973 (EPA, NOAA, NASA, DOT, etc.).
12. Klemas, V., M. Otley, C. Wethe, and R. Rogers, ERTS-1 Studies of Coastal Water Turbidity and Current Circulation, American Geophysical Union Annual Meeting, Washington, D.C., April 8-12, 1974.
13. Klemas, V., M. Otley, W. Philpot, and R. Rogers, Correlation of Coastal Water Turbidity and Circulation with ERTS-1 and Skylab Imagery. Proceedings Ninth International Symposium on Remote Sensing of Environment, April 15-19, 1974, Ann Arbor, Michigan.
14. Klemas, V., D. Bartlett, and R. Rogers, Inventories of Delaware Coastal Vegetation and Land Use Utilizing Digital Processing of ERTS-1 Imagery. Proceedings Ninth International Symposium on Remote Sensing of Environment, April 15-19, 1974, Ann Arbor, Michigan.
15. Klemas, V., F. Daiber, O. Crichton, and A. Fornes, Inventory of Delaware's Wetlands. Photogrammetric Engineering, Vol. XV, No. 4, April, 1974.
16. Klemas, V., J. Borchardt, L. Hsu, G. Gredell, and H. Wang, Photo-Optical Determination of Shallow-Water Wave Spectra. Proceedings International Symposium on Ocean Wave Measurement and Analysis, New Orleans, Louisiana, September 9-11, 1974.
17. Klemas, V., D. Maurer, W. Leatham, P. Kinner, and W. Treasure, Dye and Drogue Studies of Spoil Disposal and Oil Dispersion. Journal of Water Pollution Control Federation, Vol. 46, No. 8, August, 1974, pp. 2026-2034.
18. Klemas, V., D. Bartlett, W. Philpot, and R. Rogers, Coastal and Estuarine Studies with ERTS-1 and Skylab. Remote Sensing of Environment, 3, 153-174, 1974.
19. Klemas, V., D. Bartlett, and R. Rogers, Coastal Zone Classification from Satellite Imagery. Photogrammetric Engineering and Remote Sensing, Journal of the American Society of Photogrammetry, Vol. 41, No. 3, April, 1975.
20. Klemas, V., G. Davis, H. Wang, W. Whelan, and G. Tornator, A Cost-Effective Satellite-Aircraft-Drogue Approach for Studying Estuarine Circulation and Shelf Waste Dispersion. Proceedings Ocean 75 Conference, San Diego, 1974.

21. Klemas, V., Remote Sensing of Wetlands Vegetation and Estuarine Water Properties. Proceedings Third International Estuarine Research Conference, Galveston, October 6-9, 1975 (Invited Paper).
22. Tayfun, M. A., C. Y. Yang, V. Klemas, and H. Wang, Analysis of Inhomogeneous Wave Number Spectra. Journal of Geophysical Research, Vol. 80, No. 24, 1975.